The Potential for Fuel Reduction to Offset Climate Warming Impacts on Wildfire Intensity in California

Patrick T. Brown[1,2,3]*, Scott J. Strenfel[4], Richard B. Bagley[4], Craig B. Clements[2,5]

[1]Climate and Energy Team, The Breakthrough Institute, Berkeley, California

[2]Wildfire Interdisciplinary Research Center (WIRC), San José State University

[3]Energy Policy and Climate Program, Johns Hopkins University

[4]Meteorology Operations and Fire Science division, Pacific Gas and Electric Company, Oakland, California

[5]Department of Meteorology and Climate Science, San José State University

*Corresponding author. Email: Patrick@thebreakthrough.org

A pre-peer-reviewed preprint

Increasing fuel aridity due to climate warming has and will continue to increase wildfire danger in California[1-4]. In addition to reducing global greenhouse gas emissions, one of the primary proposals for counteracting this increase in wildfire danger is a widespread expansion of hazardous fuel reductions[5,6]. Here, we quantify the potential for fuel reduction to reduce wildfire intensity using empirical relationships derived from historical observations using a novel combination of spatiotemporal resolution (0.5km, hourly) and extent (48 million acres, 9 years). We use machine learning to quantify relationships between sixteen environmental conditions (including ten fuel characteristics and four temperature-affected aridity characteristics) and satellite-observed fire radiative power. We use the derived relationships to create fire intensity potential (FIP) maps of sixty historical weather snapshots at a 2km and hourly resolution. We then place these weather snapshots in differing background climatological temperature and fuel characteristic conditions to quantify their independent and combined influence on FIP. We find that in order to offset the effect of climate warming under the SSP2-4.5 emissions scenario, fuel reduction would need to be maintained perpetually on ~3 million acres (at a 5-year return frequency, 600,000 acres, or ~1% of our domain, per year) by 2050 and ~8 million acres (at a 5-year return frequency, 1.6 million acres, or ~3% of our domain, per year) by 2090. Overall, we find substantial potential for fuel reduction to negate the effects of climate warming and that whether or not fuel reduction is scaled up has larger leverage on our domain average FIP than shifting global greenhouse gas emissions from the SSP2-4.5 to the SSP1-2.6 trajectory.

Main

Annual area-burned in the Western United States and in California saw a precipitous decline from the 1800s to the 1980s[7-9] but has since been on an ascent[10-12]. The increase in fire activity over the recent several decades has led to increased impacts, with total annual economic burdens from wildfires in California now estimated to be over 100 billion $USD per year[13,14]. In addition to warming-induced increases in fuel aridity[1-4], fire impacts are being enhanced by a myriad of direct human influences[15,16], including changes in ignition patterns[17-19], more structures in harm's way[20], and the long-term buildup of fuels[21-23] partially due to the legacy of ill-advised policies that suppressed natural fires and eliminated the cultural burning of indigenous people[5,24,25]. Fire danger outside of forested regions is also a major concern, as fires emanating from shrublands and grasslands are responsible for more destroyed structures in the United States than those emanating directly from forests[20].

Fires are natural and inevitable[26], but fuel reduction has the potential to reduce fire intensity and smoke emissions, reduce fire severity, increase ecosystem resilience and health, and make it easier to contain fires[5,24]. Thus, one of the primary proposed strategies to address warming-induced increases in wildfire danger in California is a substantial expansion of intentional fuel removal, which includes mechanical thinning and prescribed burning in forests[5,6] and prescribed burning and enhanced grazing[27] in shrublands and grasslands[28].

There is substantial evidence that fuel reduction can be effective at mitigating wildfire risk[24,29], but studies to date tend to be on small scales, for particular circumstances (e.g., refs.[30-35]), and it is unclear if they generalize to broad spatial scales, if they are consistent for extreme and non-extreme fire weather conditions[36] and to what degree the effects of fuel reduction could counteract projected climate warming[37]. Since scaling hazardous fuel reduction treatments to large areas in California could cost billions of $USD per year[38], there is a critical need for quantitative estimates of this strategy's potential effectiveness, especially in the face of projected future warming[39].

Ideally, process-based physical models would be used for such a quantification because causality is often easier to ascertain than it is for statistics-based models. However, processed-based dynamic vegetation climate models are not currently fit for this purpose (e.g., ref.[40]; Section S22 of ref.[3]).

In lieu of using process-based physical models, we use a data-driven machine-learning approach that builds on the methods of ref.[3] but improves on them along several dimensions (Extended Data Table 1). The approach can be summarized in three steps (more details in Methods):

1. **Learn relationships between environmental conditions and fire intensity:** We combine high-resolution granular fuel data, weather data (Extended Data Table 2), and remotely sensed fire data to empirically quantify, via machine learning, the relationships between environmental conditions, fuels and Fire Radiative Power (FRP) - a proxy for fire size, biomass combustion rates[41], emissions of smoke and particulate matter[42-44], spread rates[45], intensity[46], and overall fire severity/impacts[47,48].
2. **Extrapolate in space:** We use the derived relationships to create Fire Intensity Potential (FIP) maps for most of California at hourly resolutions (snapshots in time) for a selection of hours from our historical dataset.
3. **Make future projections:** We place the historical weather snapshots in different combinations of background warming and fuel characteristic conditions (designed to represent the expected effects of climate change and fuel reduction treatments) to assess how FIP changes.

Step 1 is expounded upon in the Methods section. Figure 1 illustrates Step 2, and Figs. 2-4 illustrate Step 3.

Figure 1a shows the selection of the hourly weather snapshots that serve as the focus of our analysis. We conduct the investigation at the hourly resolution because that is the native resolution of our datasets, and it allows us to create operational fire danger forecasts at the hourly resolution (SJSU-PG&E 2 KM WRF Model Fire Models), which can inform daily operational decisions and can be used to investigate climate change affects that are a function of the diurnal cycle (an important emerging research topic[46]).

The tradeoff for retaining the hourly resolution is that computational and memory constraints limit the number of hourly maps that can be placed in different background climate and fuel conditions (each map has 48,606 locations).

Under these practical constraints, we chose a study design that compares results for thirty hourly maps that represented potentially extreme fire weather conditions and thirty hourly maps that represented more typical fire weather conditions (thus, we investigate 48,606×60=2,916,360 location-hours). The primary reason to separate data into extreme and typical fire weather conditions is that there are questions about whether the effects of warming, as well as the effects of fuel reduction may be different depending on the extremity of the fire weather (e.g., how fast the winds are[26,36,37]).

The thirty potentially extreme fire weather hours were selected based on their consequences in terms of having the highest statewide total FRP in our dataset. We also applied the additional criterion that hours were separated from each other by at least four days so that they represented relatively independent synoptic weather events (red dots in Fig. 1a). The thirty randomly selected weather snapshots, designed to sample more typical fire-weather conditions, are shown with blue dots.

Figure 1b-d shows the machine-learning model predicted Fire Intensity Potential (FIP) maps for three historical weather snapshots with the most domain-wide FRP (FRPs of individual fires are shown with magenta dots within the map). The snapshot with the highest FRP occurred on September 8th, 2020, where FIP was calculated to be highest in the forested mountainous regions of Northern California (Fig. 1b).

The two snapshots with the next most FRP (August 19th and September 16th, 2020) exhibited the highest FIP in the Western Sierra Nevada foothills near the transition between forest and shrublands (See inset in Fig. 4d for a map of land surface types). The three random snapshots (Fig. 1e-g) show mean FIP well below those of the consequential hours, with some diversity between them but with the highest FIPs again tending to be in the Western Sierra Nevada foothills near the transition between forest and shrublands.

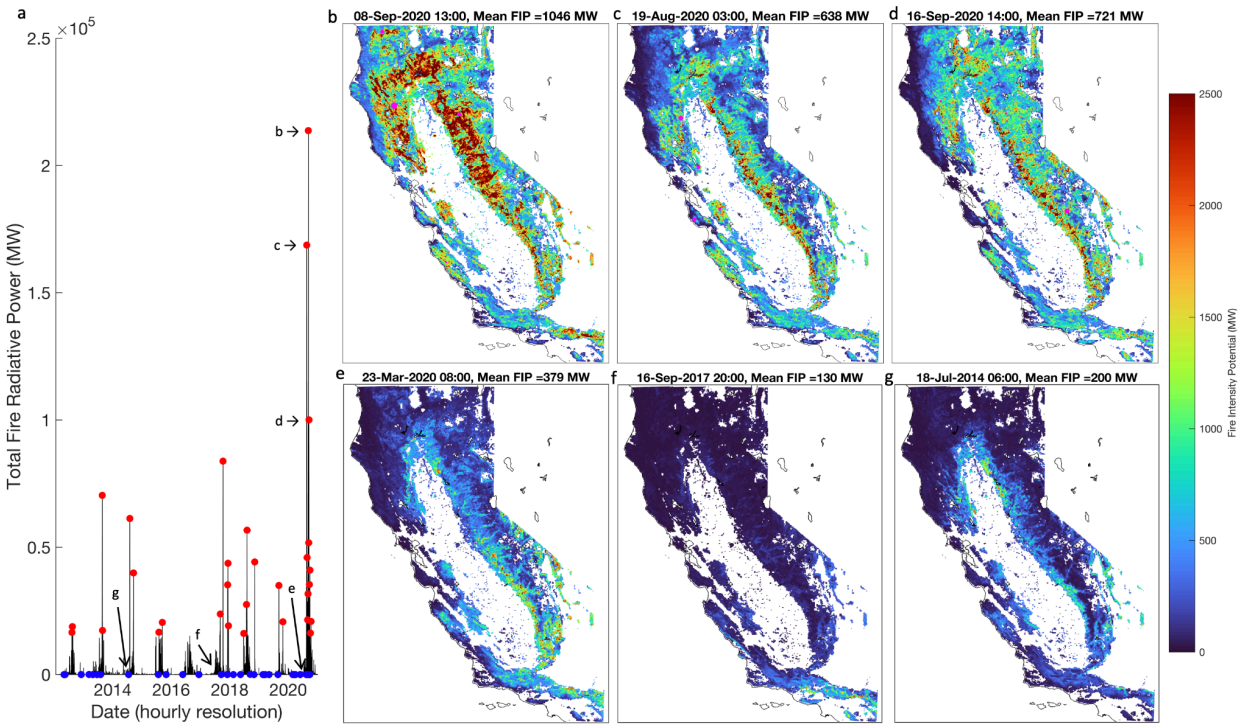

Fig. 1: Selected weather snapshots and the machine-learning model predicted Fire Intensity Potential (FIP) for six of those snapshots. a, total observed fire radiative power in the domain at an hourly resolution (black line) with the thirty highest values (separated by at least four days) shown with red dots and thirty randomly selected snapshots shown with blue dots. **b-d**, FIP maps for the three hours with the largest fire radiative power (locations of fires are shown with magenta dots). **e-g**, FIP maps for three hours from the random pool.

Figures 2-4 show how FIP may change under climate warming scenarios using the machine learning models (Extended Data Fig. 1) and fuel reductions (Extended Data Fig. 2), given the historically-observed relationships.

Because we are interested in the *potential* for fuel reduction to counteract climate warming, without being overly concerned about practical constraints, we show results for the bounding case of universal hazardous fuels reduction (Extended Data Fig. 2, Figs. 2-4) but complement this with results as a function of the area that undergoes fuel reductions (Fig. 4, Extended Data Figs. 3-4).

The spatial pattern of FIP for the most consequential snapshots (Fig. 2a) is reminiscent of the 2nd and 3rd most consequential hours in the dataset (Figs. 1c and 1d). Overall, the mean map (Fig. 2a) is fairly representative of the individual hours that constitute it (the mean spatial correlation between the individual hour maps and the mean map is r=0.81). The highest FIPs tend to be seen in the mid-elevation forested regions of the western slope of the Sierra Nevada, the Klamath ranges, and the inner North Coast ranges. FIP is generally higher in the lower elevation hardwood forests[48], near the transition to shrubland, as opposed to the higher elevation conifer forests. There are also local FIP maxima in parts of the Central Coast Ranges,

the San Gabriel Mountains, the grasslands of the southern foothills of the Sierra Nevada, and in the chaparral of the Southern Mountains.

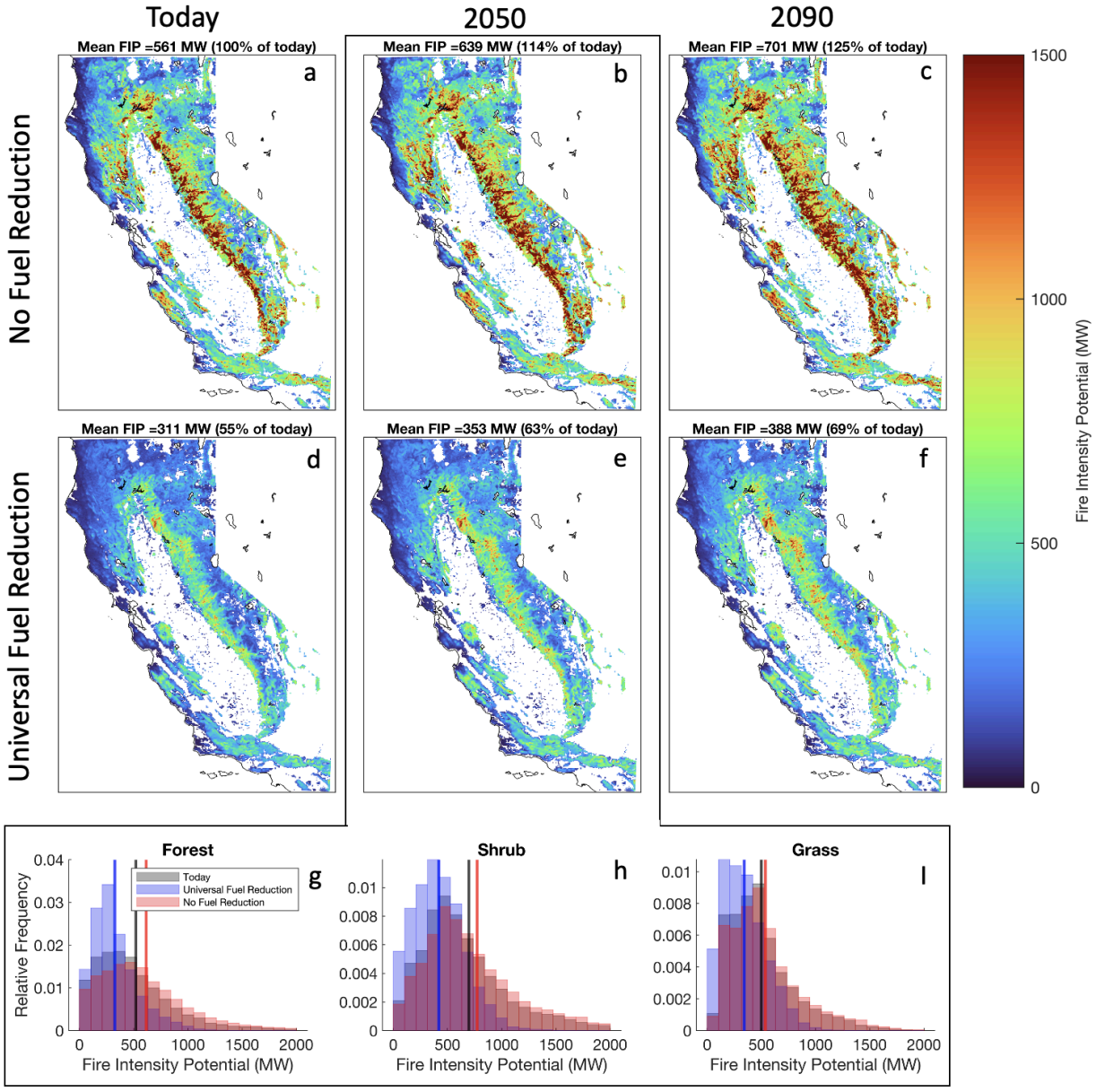

Fig. 2: Mean Fire Intensity Potential (FIP) for the most consequential weather snapshots and the effect of fuel reductions and warming associated with the SSP2-4.5 emissions scenario. a, Mean FIP map under the current climate. **b,c** Mean FIP map under 2050 warmth and under 2090 warmth in the SSP2-4.5 scenario (see Methods, Extended Data Fig. 1). **d-e**, Same as a-c but under the universal fuel reduction scenario (see Methods, Extended Data Fig. 2). Differences from today are shown in Extended Data Fig. 3. **g-i,** Distributions (across space) of FIP values under the climate change and fuel reduction conditions in 2050 for three main fuel types.

As aridity increases due to warming associated with the SSP2-4.5 emissions scenario (Fig. 2b-c), the FIP spatial pattern remains consistent but is enhanced, with mean increases in FIP of 14%

under 2050 temperatures and 25% under 2090 temperatures. The largest increases in FIP tend to be seen in forested regions, followed by shrublands and grasslands (Fig. 2g-i). The consistency of the spatial pattern under the three temperature conditions suggests that the areas of highest fire danger today will remain the same in the future largely because the spatial variation in FIP is much larger than the climate change-induced change in FIP over the time period.

Universal fuel reduction applied under today's temperature conditions results in a nearly universal reduction in FIP (Extended Data Fig. 3) with a domain-mean FIP of 55% of today's (Fig. 2d). As aridity increases due to warming, under the universal fuel reduction condition (Fig. 2e, 2f), the FIP spatial pattern again remains consistent but is enhanced, with domain mean FIPs of 63% of today's value under 2050 temperature conditions and 69% of today's value under 2090 temperature conditions. Fuel reduction has the most impact in shrublands followed by forest and grasslands (Fig. 2g-i).

The corresponding results for the thirty random snapshots are very similar, but all on a lower baseline FIP (Fig. 3). The individual hours are less consistent with each other than they are in the consequential case: the mean spatial correlation between the individual hour maps and the mean map is r=0.59. Nevertheless, the spatial correlation between the mean FIP maps for the thirty consequential and thirty random snapshots (Fig. 2a and Fig. 3a) is r=0.94. Overall, the similarity between Fig. 2 and Fig. 3 indicates that the influence of changes in temperature and changes in fuel characteristics on FIP is not dependent on the baseline conditions being extremely conducive to wildfires but rather is consistent over a wide range of conditions.

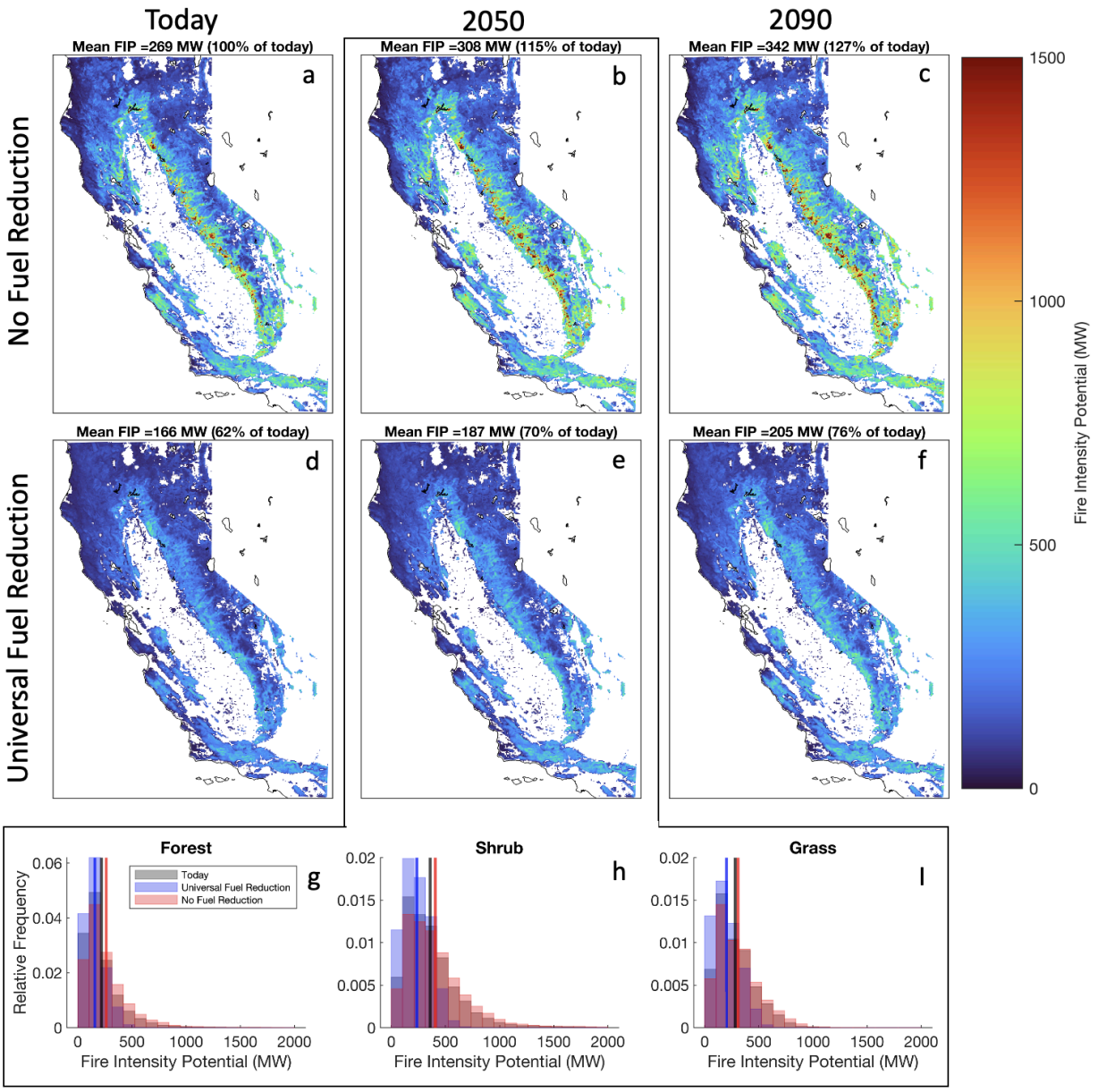

Fig. 3: Same as Fig. 2 but for the randomly selected weather snapshots.

The universal fuel treatment scenario shows substantial potential to offset the fire-danger-enhancing effects of warming but should be considered a bounding case quantifying the maximum potential for fuel reduction to counteract climate warming. However, the efficacy of fuel reduction is disproportionately large in specific regions, and thus, targeting those regions for fuel reduction would have a disproportionally large influence on domain-mean FIP. Extended data Figs. 3 and 4 show FIP changes for scenarios where fuel reduction is maintained perpetually on 1 million, 2 million, 4 million, and 8 million acres, corresponding to 2%, 4%, 8%, and 17% of our domain, respectively.

Fuel reduction should be effective in forests for at least six years[48] but could last for 20 years[49]. In shrublands, the effect should last at least five years[50]. If we assume fuel reduction would need to be maintained at a frequency of once every five years on average, the above scenarios would correspond to treatment rates of 200,000 acres per year (0.4% of our domain), 400,000 acres per year (0.8% of our domain), 800,000 acres per year (1.7% of our domain), and 1,600,000 acres per year (~3% of our domain), respectively. These rates are within the range of plausibility, given that 1 million acres per year is the stated near-term goal in California[6].

Under 2050 temperatures in the SSP2-4.5 scenario, maintaining targeted fuel treatment on 1 million acres halves the increase in FIP from warming from 114% of today's value to 107% of today's value (Extended Data Fig. 4). Maintaining targeted fuel treatment on 3 million acres completely offsets the increase in FIP from warming. If fuel reduction were maintained on 8 million acres, FIP would be reduced by roughly 12% relative to today.

Under 2090 temperatures in the SSP2-4.5 scenario, maintaining targeted fuel treatment on 2 million acres halves the increase in FIP from warming from 125% of today's value to 113% of today's value (Extended Data Fig. 4). Maintaining targeted fuel treatment on 8 million acres completely offsets the increase in FIP from warming. More than 8 million acres would have to be maintained to reduce FIP relative to today, under 2090 conditions.

Figure 4 summarizes these results and puts them in the context of the effects of shifting global greenhouse gas emissions from the SSP2-4.5 scenario to the SSP1-2.6 scenario.

Fuel treatment on 8 million acres (1.6 million acres per year at a return interval of once every five years) reduces FIP the most where it is highest today, in the transition region from the forest into shrubland (green to yellow to orange in the inset in Fig. 4d). Additionally, fuel reduction has a high impact in grass-dominated regions (Fig. 4b and Fig. 4d).

Overall, the difference in FIP between conducting fuel reduction on 8 million acres or not is much larger than the difference between the emissions scenarios, especially in 2050. This is notable because the SSP1-2.6 rapid emissions reduction pathway is roughly in line with the "below 2.0°C" goal of the Paris Agreement target (mean 2100 global warming expected to be ~1.7°C) while the SSP2-4.5 emissions pathway does not see global emissions peak until the 2040s, and a central estimate of warming by 2100 is ~2.6°C[51]. The movement from an SSP2-4.5 emissions scenario to an SSP1-2.6 scenario thus likely represents major differences in the global energy and agricultural economies, technology adoption, geopolitics, etc.[52]. Yet, these differences translate into only marginal changes in California mean FIP, especially over the next several decades (i.e., under 2050 climate). For example, in 2050, movement from the SSP2-4.5, no fuel treatment scenario to the SSP1-2.6, no fuel treatment scenario reduces the FIP increase only marginally from 114% to 112% of today's value (Fig. 4a) for the most consequential snapshots or 115% to 112% of today's value for the random snapshots. However, movement from the SSP2-4.5, no fuel treatment scenario to the SSP2-4.5, 8 million acre scenario (1.6 million acres per year at a return interval of five years) reduces the FIP increase from 114% to 88% of today's value (Fig. 4a) for the consequential snapshots and 115% to 91% of today's value for the random snapshots (Fig. 4b). Thus, these results indicate that over the next several decades, whether or

not fuel reduction treatment is scaled up has much more leverage on wildfire risk in California than whether or not global policies dictate the achievement of international emissions targets.

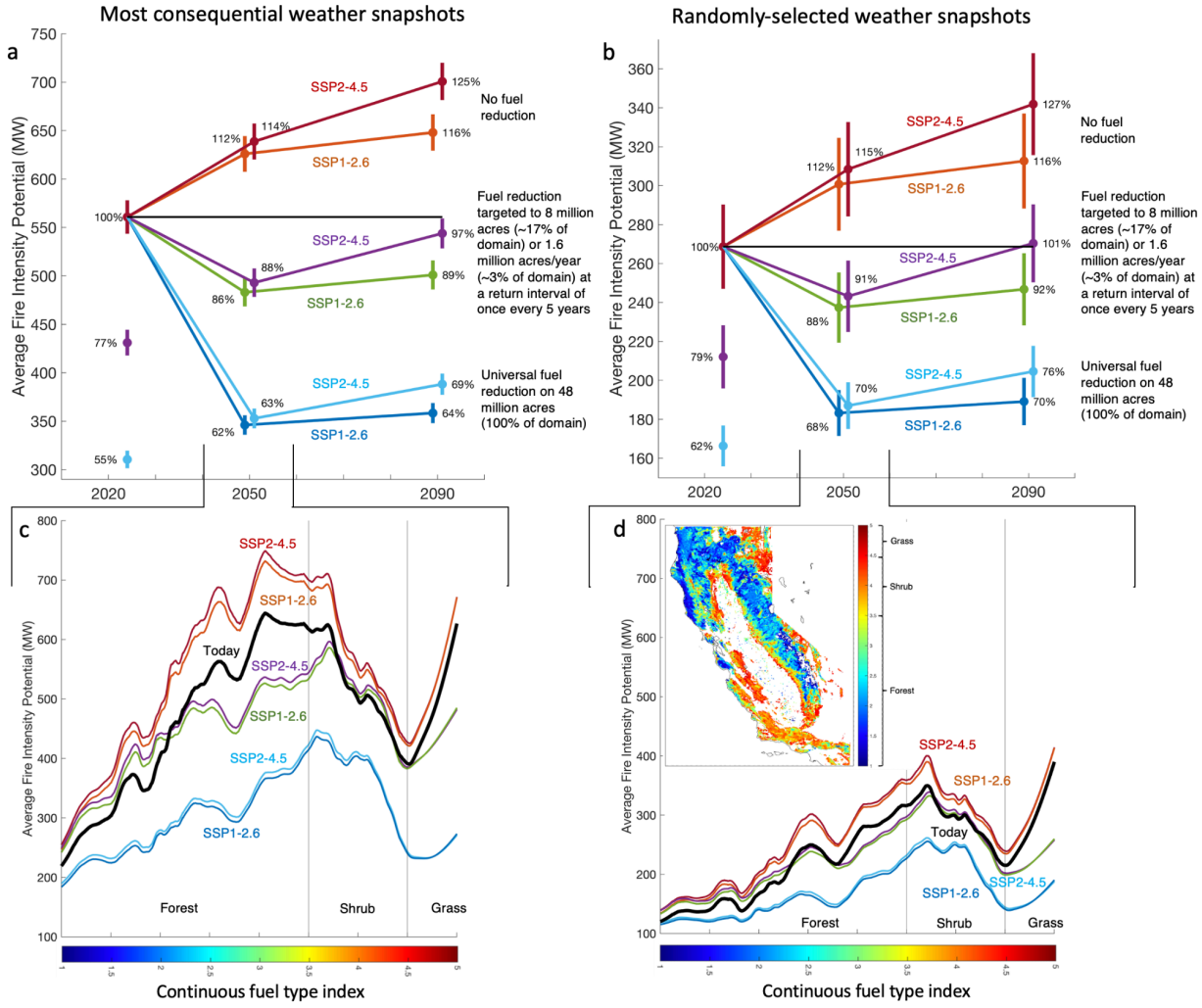

Fig. 4: Change in map-mean Fire Intensity Potentials (FIPs) under various climate and fuel reduction scenarios. a, for the most consequential weather snapshots, and **b**, for the randomly selected weather snapshots. Error bars are standard errors in the domain-mean FIP values across the thirty snapshots. **c**,**d**, FIPs under the various scenarios as a function of a continuous surface fuel type index (shown in space in the map in panel **d**, see also Methods). Maps of the predictor variables and how they are altered in the climate change and fuel reduction scenarios are shown in Extended Data Fig. 1 and Extended Data Fig. 2.

These results come with a number of important caveats (many of which are expounded upon in the Methods section). One is that the representations of both fuel reduction as well as climate change are relatively simple. The climate change scenarios only consider warming's impact on aridity, keeping constant, for example, absolute humidity, wind, and antecedent precipitation (discussed in depth in ref.[3]). The fuel reduction scenarios are represented in a stylized way (Methods), and future fuel changes do not take into consideration any further fuel accumulation, other anthropogenic land use changes[53], or any response of vegetation to climate change[54,55] or to fires[56]. Another important caveat is that we have only investigated sixty

historical weather snapshots here (though this represents 48,606×60=2,916,360 location-hours). Despite this limited number, we interpret the consistency between the consequential and randomly selected set of snapshots (cf. Fig. 2 and Fig.3; cf. Fig. 4a and Fig. 4b) as evidence that our results hold across a wide range of weather conditions. Finally, an important caveat is that we have not taken into consideration any practical impediments to implementing fuel reduction, which include physical impediments (e.g., the slope of topography, accessibility, finding appropriate burn windows for prescribed fire[57]), cultural and political opposition to mechanical thinning and prescribed burning[58], and federal regulations[15]. These barriers would curtail the ability of fuel reduction scenarios to reduce FIP. On the other hand, studies have shown that much of the wildfire mitigation benefits of fuel reduction can be achieved by treating only a strategic portion of the land[29,59-65] which might indicate that the stated areas in our targeted fuel treatment scenarios are higher than would actually be necessary to achieve the calculated effect.

These caveats notwithstanding, the findings here add to a large and growing body of literature that suggests a substantial potential for hazardous fuel reduction to mitigate wildfire risk in California and elsewhere[29-35,48,59,66-69]. At plausible fuel treatment rates, the impact of warming-induced aridity increases on average fire intensity potential could be negated for the remainder of the century, even in an SSP2-4.5 emissions scenario. Also, whether or not fuel reduction is scaled to stated goals has larger leverage on average fire intensity potential than shifting global greenhouse gas emissions from the SSP2-4.5 to the SSP1-2.6 trajectory.

Methods

Overview

We seek to empirically quantify the potential effectiveness of widespread hazardous fuel reduction treatments on wildfire danger in the face of continued increases in fuel aridity due to climate warming.

Our methodology builds on the methods of ref.[3] and is conceptually very similar (See Fig. 1 in ref.[3]) but improves on it along several dimensions (Extended Data Table 1). The main advancement is that in ref.[3], we take weather sequences associated with 17,910 fire days and place them in six different climatological temperature conditions, whereas, in the present study, we take weather sequences associated with 2,916,360 hours (60 hours × 48,606 locations) and place them in eighteen different scenarios representing changes in climatological temperature *and* fuel characteristics. The result is that this study evaluates ~489 times more data points than ref.[3].

We use machine learning models (specifically neural networks and random forests) and historical data to quantify the relationships between environmental conditions (predictors) and fire radiative power (FRP, our response variables). Many traditional regression methods assume that the influence of any predictor variable is independent of the influence of the other predictor variables and that their influences are monotonic, if not linear. However, it is well known that the influence of any one of our predictor variables (Extended Data Table 2) will be highly conditional on the state of the other predictor variables. Thus, rather than use traditional regression methods, we use machine learning models (applied similarly in other related research[3,70-74]) that are able to account for non-linear, non-monotonic, and interactive relationships between the predictors without the researcher having to presuppose the functional forms of such relationships.

Once the relationships are learned (encapsulated in the trained models), we make maps of Fire Intensity Potential (FIP) for various hourly weather snapshots from our historical dataset. Then, we take these hourly snapshots and alter background temperature (aridity) and physical fuel characteristics to quantify the effect of warming and hazardous fuel reduction treatments on FIP for those weather snapshots.

We use a novel (and, to our knowledge, unprecedented) combination of spatial resolution (0.5km, the resolution of the VIIRS satellite[75,76], temporal resolution (hourly, the resolution of a dynamically downscaled WRF reanalysis), spatial extent (4.8 million acres in our spatial domain), temporal extent (9 years, 2012-2020), number of instantaneous fire observations (27,289) and granularity of fuel characteristics (6 attributes of surface fuels and 4 attributes of forest canopy from LandFire[77] to conduct our assessment.

Other research has been conducted using conceptually similar statistical modeling approaches at annual[2], monthly[70,78], or daily[3,79] resolutions, but here we conduct analysis at the hourly resolution, which is the native resolution of our dataset. One advantage of using the hourly resolution is that it allows for inferences to be made on conditions that can vary substantially over the diurnal cycle[46] (e.g., low 1-hour dead fuel moisture occurring simultaneously with high

wind speeds). This is a key advantage because there are questions about whether fuel reduction is as effective under the most extreme fire weather conditions as it is under more moderate conditions[37,80]. Another motivation to focus on the hourly timescale is that a primary goal of this work is to support an operational fire danger forecast model at an hourly resolution (SJSU-PG&E 2 KM WRF Model Fire Models, http://www.met.sjsu.edu/weather/wirc-prod/maps/frpMaps.html) that can help inform decisions for the forthcoming day(s) like the issuance of red-flag warnings, the allocation of firefighting resources, or the application of de-energization of powerlines. The tradeoff for retaining the hourly resolution is that computational and memory constraints strongly constrain the number of hours that can be investigated (this study evaluates ~489 times more data points than ref.[3]).

Predictor variables

We use sixteen environmental conditions as predictor variables (Extended Data Table 2). They consist of one topographic characteristic (slope), ten fuel characteristics (e.g., fuel loads and canopy characteristics), four weather and climate-influenced fuel aridity measures (1, 10, 100, and 1000 hour dead fuel moisture, DFM), and one additional weather characteristic (wind). These predictors represent components of the canonical "wildfire behavior triangle"[81] that can be broken into topography, fuels, and weather.

Topography Characteristics

In the wildfire behavior triangle, it is typical to represent topography with slope, elevation, and aspect, but we use only slope. This is because the influence of elevation and aspect on fire danger is primarily through their influences on fuel characteristics (e.g., fuels change dramatically on the northward vs. southward facing slopes and change dramatically as a function of elevation). Since fuel characteristics are represented independently (see below), it would be redundant and inappropriate for our study design to include aspect and elevation as predictor variables. The slope is included as its own predictor because it has an influence on fire behavior independent of fuels - allowing for the more efficient preheating of fuels in the upslope direction[82].

Fuel Characteristics

Hazardous fuel reduction treatments seek to reduce surface and canopy fuel loads and alter other characteristics like canopy base height[64]. Thus, we seek data that represents these characteristics so that they can be altered in our fuel reduction scenario. For forested regions, we represent the forest canopy structure with the four variables that are provided for this purpose from the Landfire dataset[77,83] (Extended Data Table 2). We use LandFire 2012 in our model training (which trains on fires from 2012 to 2020) and LandFire 2020 as the basis for our future scenarios.

Some characteristics of surface fuel loads can be estimated directly via remote sensing[84], and promising quantifications are on the horizon[85]. However, there are no direct estimates of most of the characteristics we seek to alter in our fuel reduction scenarios. Thus, we estimate six surface fuel characteristics from their Scott and Burgan surface "fire behavior fuel model" category[86].

Specifically, we take each location's Scott and Burgan category (FBFM40) and assign that location six surface fuel values based on the standard value obtained from Table 7 in ref.[86]. Thus, we use Scott and Burgan categorical data in this study, but only to assign physical fuel characteristics to a location. Our machine learning models never receive direct information on the FBFM40 category. This was because we wanted the machine learning models to be trained only on continuous physical characteristics so that results could be as interpretable as possible and causality could be plausibly inferred from, e.g., partial dependence relationships (Extended Data Fig. 6).

A major caveat that might make our results conservative (i.e., may make it so that we underestimate the influence of fuel reductions) is that the above procedure is an indirect and imprecise estimate of fuel characteristics. Any errors in these estimates would add noise to the quantification of the relationship between fuel characteristics and fire intensity and would thus reduce the leverage of the fuel reduction scenario.

Weather and Climate Characteristics

Typically, the weather's influence on fire danger is represented by the degree to which it is "hot, dry, and windy." and predictors like temperature, precipitation, humidity, and wind speed are often used (e.g., ref.[78]). Wind tilts flames into fuels, provides oxygen, aids in heat transfer, and carries hot embers and firebrands ahead of the main fire, causing spot fires[82]. Thus, in our analysis, wind serves as its own independent predictor.

The "hot and dry" components are combined and decomposed by their influence on fuels as a function of timescale. This was done because air temperature affects fire danger primarily via increasing saturation vapor pressure (lowering the relative humidity) and thus reduced moisture content of fuels[87] but as a strong function of the size of those fuels and thus how long conditions are sustained[88]. We thus combine the "hot" and "dry" influences of the weather/climate by calculating 1-hour, 10-hour, 100-hour, and 1,000-hour dead fuel moisture (in the same way as in ref.[3]). The calculations incorporate temperature, relative humidity, and precipitation over 3,000 hours (125 days) of antecedent conditions since this represents the period over which 1,000-hour dead fuel moisture would reach ~95% of its equilibrium value. The fact that these four measures are collinear does not present a problem for our study design because we do not seek to quantify any one of their independent influences on the response variable; instead, warming is propagated into all four variables simultaneously in the climate change scenarios.

Response variable

The fire characteristic that we focus on, serving as our response variable, is geolocated instantaneous Fire Radiative Power (FRP) in megawatts (MW) within California state lines obtained from the Visible Infrared Imaging Radiometer Suite (VIIRS) instrument[75] on the Suomi National Polar-orbiting Partnership (Suomi NPP) satellite. The raw satellite data was processed according to procedures laid out in ref.[76].

FRP quantifies a fire's radiant energy release rate and is associated with the fire's size and fireline intensity (i.e., power per unit length of the firefront). It thus serves as a proxy for fire

intensity[46] and biomass combustion rates[41] and a more indirect proxy for emissions of smoke and particulate matter[42-44], fire spread rates[45], and overall fire severity/impacts[47,48].

FRP is a useful response variable in our context because the aim of fuel management practices is not to eliminate fires but to reduce their intensity, spread rates (thereby making containment easier), and overall impacts when they do occur.

Assignment of predictor variables to response variable

Our starting point for our response variable was 27,289 instantaneous geolocated FRP observations within California state lines spanning the period 2012-2020[76]. Each FRP detection has an associated latitude, longitude, and fire size. We assigned topographic and fuel characteristics to each of these 27,289 FRP values by averaging the 30m resolution values from LandFire (version 2012, corresponding to the start of the time period) over the size of the fire, centered on the fire detection's latitude and longitude.

There was no time dimension for the topographic and fuel characteristics. We did not use different LandFire versions over the course of the training period because we wanted the derivations of fuel characteristics to be stationary over the training period. This would not be the case if multiple LandFire versions were used over the training period because each LandFire update represents an entirely new quantification of fuels using altered methods, not a simple update of how the fuels have evolved in time.

We assigned weather/climate variables to each of these 27,289 FRPs by averaging values over the size of the fire from a high resolution (2km, hourly, with 50 vertical levels) reanalysis produced by the National Center for Atmospheric Research's (NCAR) Weather Research and Forecasting (WRF) model (version 4.1.2). See Section S3 of ref.[3] for more details on the WRF reanalysis. This is the same version of WRF that is used to produce the operational version of this analysis (SJSU-PG&E 2 KM WRF Model). The dead fuel moisture calculations required 125 days or 3,000 hours of antecedent weather (precipitation and humidity). Since the time resolution of the WRF reanalysis was hourly, the hour nearest to each FRP detection was chosen to assign the weather value.

Machine learning models

Similar to ref.[3], we quantify the relationship between the predictor variables and our response variables via an ensemble of neural networks and random forest models.

Fifteen random forest models and fifteen neural network models were used. The Neural Network Models were feed-forward, fully connected, shallow neural networks produced with the function "fitrnet" built into Matlab (https://www.mathworks.com/help/stats/fitrnet.html). The random forest models were regression tree ensembles from the "fitrensemble" function built into Matlab (https://www.mathworks.com/help/stats/fitrensemble.html).

The fifteen models differed from each other in terms of their hyperparameters (Extended Data Table 4). All sets of hyperparameters were optimized via Bayesian Optimization (https://www.mathworks.com/help/stats/bayesopt.html), which seeks to minimize cross-validation loss. This was done fifteen times for each model type because Bayesian

Optimization is non-determinist and results in different final hyperparameter combinations each time. In this study, we were not attempting to maximize predictive skill but rather to make robust inferences about the influence of predictors on our response variable. Thus, all of our results use the median across all thirty models so that they represent information that is minimally conditional on the model type or on the peculiarities of specific hyperparameter combinations.

Validation

We confirm that our predictors provide information that constrains our response variable (instantaneous FRP detections for individual fires) using leave-1-year-out cross-validation, where all the FRP detections from each year in our dataset (2012-2020) are held out in sequence, the remaining data is used to train the machine learning models, and predictions are made on the year's worth of held-out data.

The results of this process are shown in Extended Data Fig. 5. The logspace correlation between instantaneous FRP predictions (median of the thirty machine learning models described in Extended Data Table 4) and observed FRP values at the level of each individual detection was r=0.5 (black dots in Extended Data Fig. 5b), with very little mean bias (centered on the 1:1 line, blue) and a p-value of effectively zero (below machine precision). This demonstrates that there is certainty that the predictors provide useful information for constraining the response variable. However, a correlation of r=0.5 means that our predictor set leaves out plenty of information that affects FRP. This would include, but is not limited to, the lifetime of the fire at the time of observation, ongoing and antecedent fire suppression efforts; high-resolution information on topography, fuels, and weather; information on tree mortality; information on the chemical makeup of fuels, information on the stability of the atmosphere and solar radiation, snow cover, etc. Also, our means of obtaining fuel characteristics via the standard values of the FBFM40 categories is indirect and imprecise.

Despite these caveats, predictive skill increases rapidly to $r > 0.85$ at higher levels of aggregation (line in Extended Data Fig. 5a). For example, the red dots in Extended Data Fig. 5b are averages of 10 FRP predictions and their associated observations, resulting in r=0.87. Aggregating in time also shows similar results. When monthly mean FRP predictions are compared to their associated observations, the correlation is r=0.9 (Extended Data Fig. 5c).

Overall, our predictor set contains incomplete information for fully determining our response variable, but it still provides useful information and thus allows us to study the influence of predictors on the response (the aim of this study).

Fire Intensity Potential (FIP) maps

After the relationships are derived, the machine learning models can predict a hypothetical FRP at any location so long as the values of all sixteen predictors are provided. The proper interpretation for these model predictions is "if a fire was active here, under these environmental conditions, this is what we would expect the FRP to be, based on historical associations." Since FRP is a proxy for fire intensity and since we are discussing the *potential* intensity *if* a fire were present, we refer to these predictions as Fire Intensity Potential (FIP).

Domain for FIP maps

The borders of our domain are defined by the WRF reanalysis used to obtain the weather variables. This reanalysis was produced to complement PG&E's Operational Mesoscale Modelling System (POMMS) and thus was centered on PG&E's service territory, excluding a portion of southeastern California (see Section S3. in ref.[3]).

Since we are studying the effects of fuel reduction on wildfire danger, we also limit our study domain to areas that could plausibly be considered for fuel reduction treatments, seeking to eliminate urban areas, California's agricultural Central Valley, and the Mojave desert. The criteria we used for this was that the 2km grid cell must have had > 2 tons per acre of surface fuels in the pre-treatment condition. This produced a spatial pattern consistent with independent estimates of land at risk of fire (e.g., ref.[89]) and also a total area very similar to that from comparable analysis conducted with other surface vegetation datasets like the California Department of Forestry and Fire Protection's (CALFIRE) Fire and Resource Assessment Program's (FRAP) 'FVEG' map[15].

Hourly weather snapshots

We conduct the investigation at the hourly resolution because that is the native resolution of our model training datasets, and it is useful to be able to investigate climatological changes in fire weather within the diurnal cycle[46]. This is particularly relevant for wind, whose important influence can be averaged out at daily and coarser temporal resolutions. Furthermore, retaining the hourly resolution allows us to create operational FIP forecasts at that resolution (SJSU-PG&E 2 KM WRF Model Fire Models), which can inform daily operational decisions.

Background climate warming and fuel reduction may have different relative effects on fire severity depending on how extreme the fire weather is (e.g., how fast the winds are[26,36,37]. Thus, we compared hourly weather snapshots for potentially extreme fire weather to randomly selected hourly weather snapshots. The potentially extreme fire weather snapshots were selected based on their consequences in terms of having the most observed FRP over the entire domain over the timespan of our dataset (Fig. 1a). In order to sample instances that represented relatively independent synoptic weather events, we included a criterion that hours be separated from each other by at least four days. We also selected thirty random hourly weather snapshots (using a random number generator) to assess the generalizability of the results.

We selected thirty snapshots for each category (sixty total) because n=30 is a common heuristic for the minimum number of observations needed to draw statistical inferences. Note, however, that this corresponds to 48,606×60=2,916,360 location-hours. We selected only thirty snapshots because of practical computational and memory constraints (as it is, this study evaluates ~489 times more data points than ref.[3]). The similarity in results between the set of the thirty most consequential hours and the thirty random hours (e.g., Fig. 4a vs. Fig. 4b) is evidence that our conclusions would not be sensitive to the inclusion of more hours.

Altered fuel and climate scenarios

Our main research goal is to assess the potential for fuel reduction to counteract climate warming. This is addressed in terms of how FIP maps for historical weather snapshots change as they are placed in different background fuel characteristics and climatological temperature conditions. The climatological temperature conditions are associated with the climate-model-calculated warming of the SSP1-2.6 and SSP2-4.5 scenarios in 2041-2060 (labeled 2050 in our study) and 2081-2100 (labeled 2090 in our study). The fuel characteristics are altered according to previously published estimates of the influence of fuel reduction treatments on those characteristics.

Climate change scenarios

Background anthropogenic warming was obtained from the Coordinated Regional Downscaling Experiment (CORDEX, https://cordex.org/). CORDEX has a 12.5km spatial resolution over our domain. Data were downloaded separately for each month of the year and as a function of space over our domain (See Fig. S21 in ref.[3]) and were bilinearly interpolated to our 2km grid. A mean temperature change was calculated from the present to 2050 and to 2090, and this warming was then translated into increases in aridity for our four aridity predictors (Extended Data Fig. 1 and Extended Data Fig. 6). This required precipitation, pressure, and absolute humidity data over the antecedent 3,000 hours (125 days) for each hourly snapshot that we investigated. See the discussion around equations S5-S10 in ref.[3] and the discussion in Section 4 of ref.[88] for further details on how temperature change is propagated into aridity change.

Universal fuel treatment scenario

We sought a simple way to alter our fuel characteristics to represent hazardous fuel reduction treatments. This alteration was intended to represent both mechanical thinning and prescribed burning in forests and prescribed burning and/or enhanced grazing in shrub and grassland. Since we derived our six surface fuel characteristics (numbered 2-7 in Extended Data Table 2) from the standard values associated with their Scott and Burgan surface "fire behavior fuel model" category (FBFM40[86]), we also altered these six surface fuel characteristics by altering their FBFM40 category. For this purpose, we follow ref.[90]. In the post-treatment condition, all surface fuel characteristics were assigned the value from the lowest Scott and Burgan surface fuel model from within that category (i.e., all GRs were assigned values corresponding to GR1, all GSs were assigned values corresponding to GS1, etc.). Since hazardous fuel treatments aim to *reduce* fuel loads, an additional criterion that no fuel loads could increase in the post-treatment condition was applied. Under the circumstances where the post-treatment condition within a category would have produced more fuel for a particular characteristic (i.e., 100-hr fuel load) than the pre-treatment condition, the pre-treatment value was retained (Extended Data Table 3). It is important to emphasize that the surface fuel characteristics are modified according to corresponding modifications to their FBFM40 category but that the machine learning models do not explicitly incorporate FBFM40 categories. This was to keep predictors as physical as possible (i.e., having continuous physical units) to maximize the interpretability of the results.

In forested areas, treatment effects on canopy characteristics were represented as proportional adjustments to their pre-treatment characteristics again following ref.[90]. In the post-treatment condition the canopy cover was reduced to 75% of its pretreatment value, canopy height, and canopy base height were increased by 20% of their pretreatment values, and canopy bulk density was decreased to 50% of its pretreatment value (Extended Data Fig. 2 and Extended Data Fig. 6).

Extended Data Fig. 6 shows the predictors ranked from one to sixteen by the magnitude of the variation of the partial dependence function (max-min). Thus, the five weather variables had the most individual impact on the machine learning model predictions of FRP, followed by the one topographic variable and then the ten fuel characteristics. Considering the partial dependence function superimposed on the fuel reduction alteration indicates that reduced fuel bed depth, reduced live herbaceous fuel load, reduced live woody fuel load, and reduced canopy bulk density make up a substantial portion of the overall effect of hazardous fuel reduction treatments.

Targeted fuel treatment scenarios

For the targeted fuel treatment scenarios of 1, 2, 4, and 8 million acres (Fig. 4, Extended Data Fig. 3, Extended Data Fig. 4), we replace non-treated 2km land grid boxes with treated grid boxes in the order of how impactful those replacements would be (i.e., for the treatment of 1 million acres, the 1 million acres where FIP decreased the most from fuel reduction were placed in the treatment condition). The calculation of where treatment had the largest impact was calculated only once under today's climate conditions (i.e., it was not recalculated for each future climate condition).

Surface fuel type index and FIP as a function of surface fuel type index

The surface fuel type index shown in Fig. 4c and Fig. 4d was calculated by assigning each 30-meter pixel (LandFire resolution) a value according to its FBFM40. These values were 1 for all timber litter pixels, 2 for all timber understory pixels, 3 for all slash-blowdown pixels, 4 for all shrub pixels, 4.5 for all grass-shrub pixels, and 5 for all grass pixels. Then, within each 2km grid box, the 4,444-pixel values were averaged together to get a single number for each 2km grid box, which is shown in the inset in Fig. 4d). The lines in Figs. 4c and 4d were calculated by ranking the 2km pixels by their continuous surface fuel type index and applying an 100-point rlowess smooth (https://www.mathworks.com/help/curvefit/smooth.html#mw_ad6b65fd-4dac-46c4-a649-a7a0b301eb80) to the associated FIP values.

Extended data figures and tables

Extended Data Table. 1: Differences between Brown et al. 2023 and this study.

Category	Subcategory	Brown et al. (2023)	Present Study
Predictor variables	Weather timescale	Daily	Hourly
	Fuel characteristics	2 variables	10 variables
	Assignment to fire at each timestep?	No, only ignition lat/lon available	Yes, new assignment for each detection
	Precipitation	Precipitation redundant as it appears as its own predictor as well as within DFM calculation	Precipitation only included within DFM calculation
Response variable	Resolution	1.5km (from MODIS)	0.5km (from VIIRS)
	Number of observations in training set	17,910	27,289
	Type of ML set up	Binary classification*	Regression on continuous variable
	Extrapolate in space	No	Yes, creating FIP maps
	Number of data points placed in different scenarios	17,910 (fire-days)	2,916,360 (60 maps, each with 48,606 locations)
Machine Learning Models	Hyperparameter optimization method	Test random combinations	Use Bayesian Optimization
	Number of hyperparameters tuned	3 for random forests and 3 for neural networks	6 for random forests and 9 for neural networks
Projections	Climate change propagation	Change in temperature inelegantly propagated into temperature itself as well as VPD and DFM predictors	Temperature elegantly propagated into only DFMs at 4 relaxation timescales
	Climate change scenarios	Include implausible RCP8.5*	Does not include implausible RCP8.5
	Climate model resolution	~1 degree (CMIP6)	12.5km (CORDEX, dynamically downscaled)
	Number of scenarios	6	36
Framing	Topic	Look exclusively at the effect of climate change*	Put effect of climate change in context of other relevant factor that could offset climate change
	Variable of study	Change in probability of crossing threshold*	Change in magnitude of response variable

Extended Data Table. 2: Sixteen predictors used in this study, their data sources and whether they were altered in the climate change and fuel reduction scenarios.

	Variable Number	Variable Name	Unit	Source	Original Resolution	Altered in Fuel Treatment Scenario	Altered in Climate Change Scenarios
Topography	1	Slope	°	LandFire	30m	No	No
Fuels	Surface Fuel Characteristics						
	2	1-hour dead fuel load	tons/acre	Scott and Burgan Standard Values via LandFire	30m	Yes	No
	3	10-hour dead fuel load	tons/acre	Scott and Burgan Standard Values via LandFire	30m	Yes	No
	4	100-hour dead fuel load	tons/acre	Scott and Burgan Standard Values via LandFire	30m	Yes	No
	5	Live Herbaceous fuel load	tons/acre	Scott and Burgan Standard Values via LandFire	30m	Yes	No
	6	Live Woody fuel load	tons/acre	Scott and Burgan Standard Values via LandFire	30m	Yes	No
	7	Fuel Bed depth	ft	Scott and Burgan Standard Values via LandFire	30m	Yes	No
	Forest Canopy Characteristics						
	8	Canopy Cover	%	LandFire	30m	Yes	No
	9	Canopy Height	m	LandFire	30m	Yes	No
	10	Canopy Base Height	m	LandFire	30m	Yes	No
	11	Canopy Bulk Density	kg/m^3	LandFire	30m	Yes	No
Weather	Temperature-affected fuel aridity						
	12	1-hour dead fuel moisture	%	WRF Reanalysis	2km, 1hr	No	Yes

	13	10-hour dead fuel moisture	%	WRF Reanalysis	2km, 1hr	No	Yes
	14	100-hour dead fuel moisture	%	WRF Reanalysis	2km, 1hr	No	Yes
	15	1000-hour dead fuel moisture	%	WRF Reanalysis	2km, 1hr	No	Yes
	Other Weather						
	16	Wind Speed	m/s	WRF Reanalysis	2km, 1hr	No	No

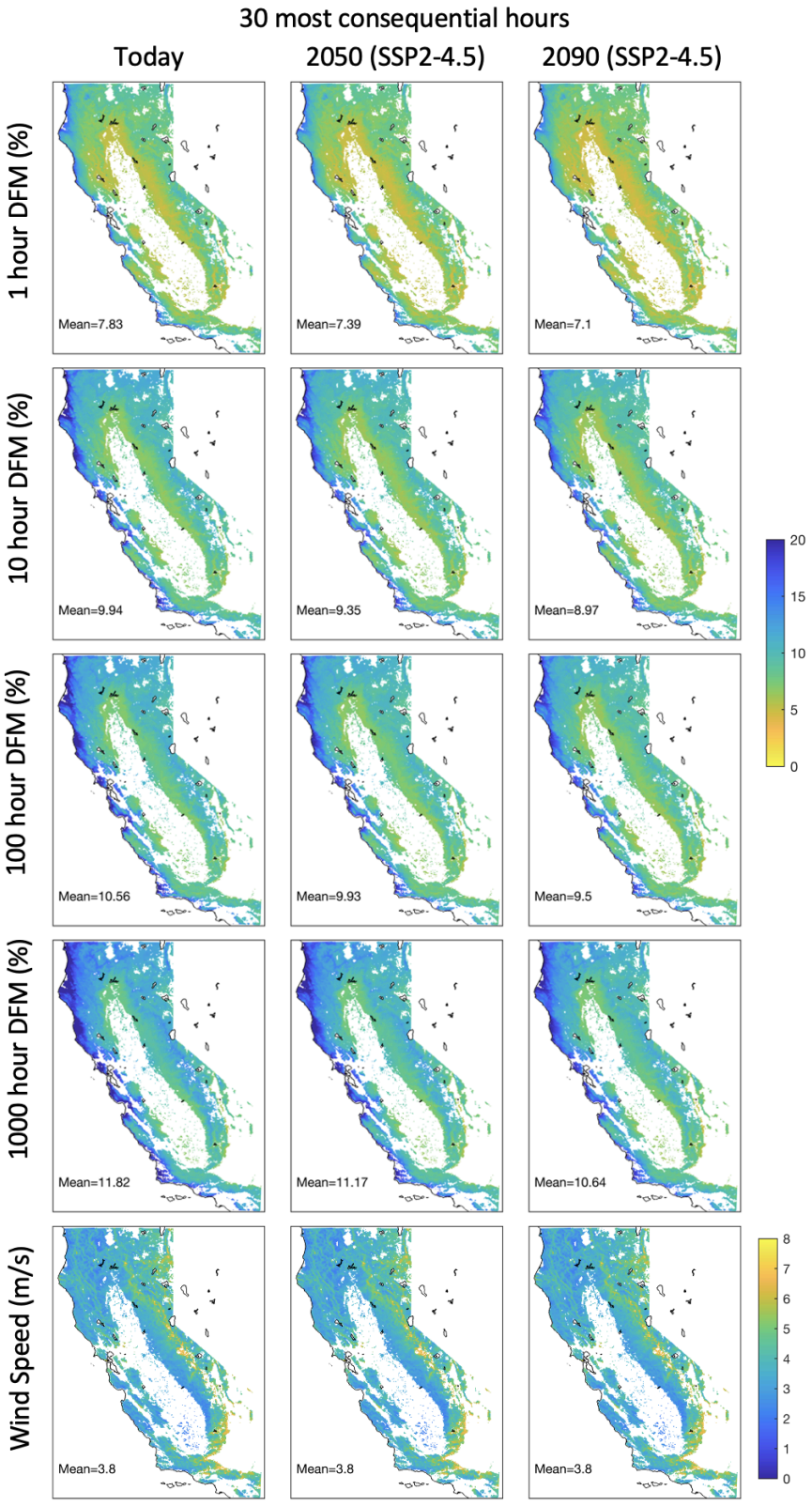

Extended Data Fig. 1: Average conditions (across the thirty consequential snapshots) for the five weather variable predictors under three background climate conditions.

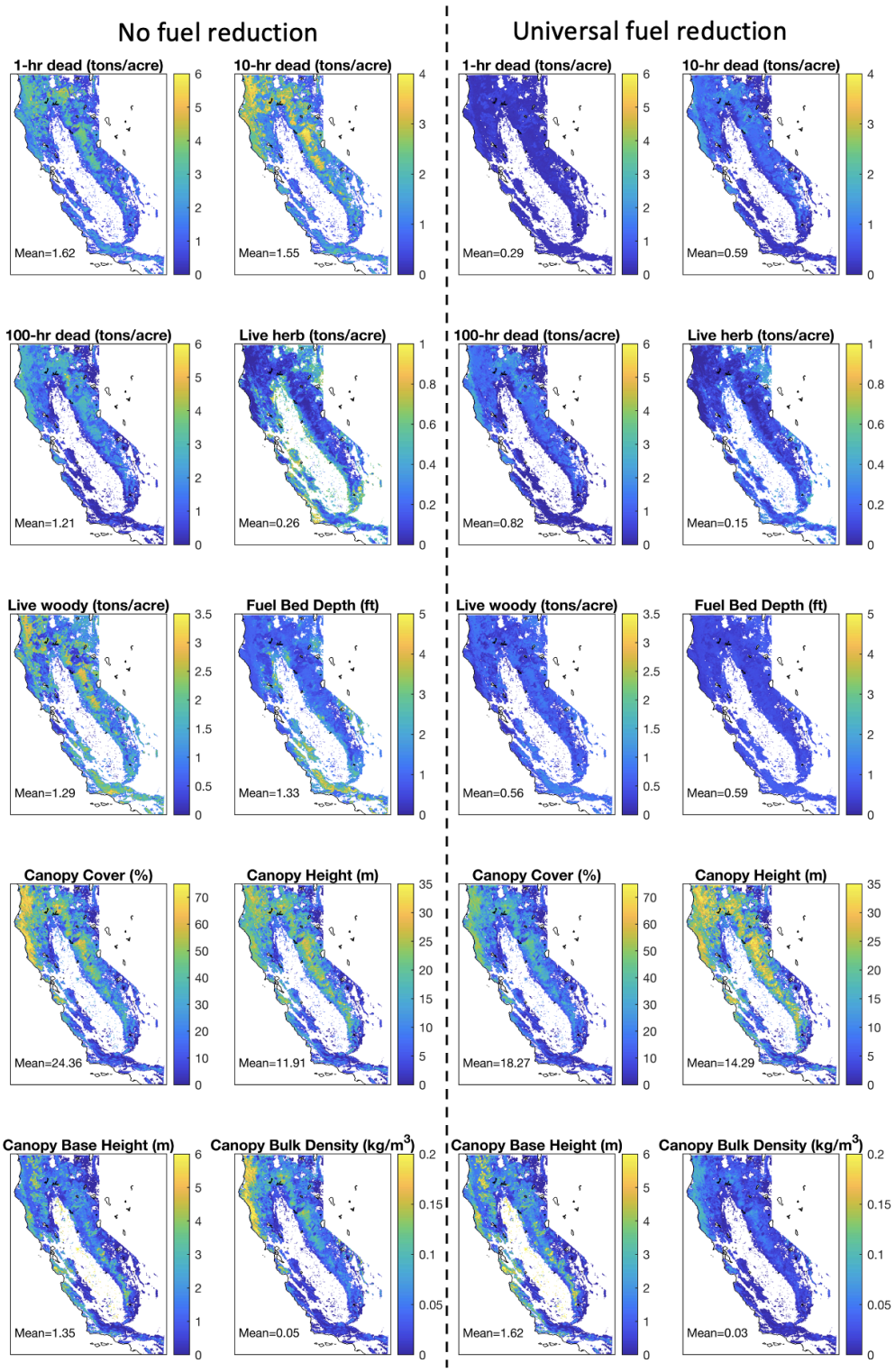

Extended Data Fig. 2: The base maps of the ten fuel characteristic predictors (left two columns) and their state after universal fuel reduction (right two columns). See Extended Data Table 3 for more details on how fuel characteristics are altered in the fuel reduction scenario.

Extended Data Table. 3: Pre-treatment and post-treatment values for the six surface fuels. In forested areas, treatment effects on canopy characteristics were represented as proportional adjustments to their pre-treatment characteristics (following ref.[90]). In the post-treatment condition, the canopy cover was reduced to 75% of its pretreatment value, canopy height, and canopy base height were increased by 20% of their pretreatment values, and canopy bulk density was decreased to 50% of its pretreatment value. See the manifestation of these alterations in maps in Extended Data Fig. 2 and in the context of predictor partial dependence function in Extended Data Fig. 6).

	Pre Treatment							Post Treatment (No increase in fuel allowed)						
Category	FBFM40 model	1-hr (t/ac)	10-hr (t/ac)	100-hr (t/ac)	Live herb (t/ac)	Live woody (t/ac)	Fuel Bed Depth (ft)	FBFM40 model	1-hr (t/ac)	10-hr (t/ac)	100-hr (t/ac)	Live herb (t/ac)	Live woody (t/ac)	Fuel Bed Depth (ft)
Grass	GR1	0.1	0	0	0.3	0	0.4	GR1	0.1	0	0	0.3	0	0.4
	GR2	0.1	0	0	1	0	1	GR1	0.1	0	0	0.3	0	0.4
	GR3	0.1	0.4	0	1.5	0	2	GR1	0.1	0	0	0.3	0	0.4
	GR4	0.25	0	0	1.9	0	2	GR1	0.1	0	0	0.3	0	0.4
	GR5	0.4	0	0	2.5	0	1.5	GR1	0.1	0	0	0.3	0	0.4
	GR6	0.1	0	0	3.4	0	1.5	GR1	0.1	0	0	0.3	0	0.4
	GR7	1	0	0	5.4	0	3	GR1	0.1	0	0	0.3	0	0.4
	GR8	0.5	1	0	7.3	0	4	GR1	0.1	0	0	0.3	0	0.4
	GR9	1	1	0	9	0	5	GR1	0.1	0	0	0.3	0	0.4
Grass-shrub	GS1	0.2	0	0	0.5	0.65	0.9	GS1	0.2	0	0	0.5	0.65	0.9
	GS2	0.5	0.5	0	0.6	1	1.5	GS1	0.2	0	0	0.5	0.65	0.9
	GS3	0.3	0.25	0	1.45	1.25	1.8	GS1	0.2	0	0	0.5	0.65	0.9
	GS4	1.9	0.3	0.1	3.4	7.1	2.1	GS1	0.2	0	0	0.5	0.65	0.9
Shrub	SH1	0.25	0.25	0	0.15	1.3	1	SH1	0.25	0.25	0	0.15	1.3	1
	SH2	1.35	2.4	0.75	0	3.85	1	SH1	0.25	0.25	0	0	1.3	1
	SH3	0.45	3	0	0	6.2	2.4	SH1	0.25	0.25	0	0	1.3	1
	SH4	0.85	1.15	0.2	0	2.55	3	SH1	0.25	0.25	0	0	1.3	1
	SH5	3.6	2.1	0	0	2.9	6	SH1	0.25	0.25	0	0	1.3	1
	SH6	2.9	1.45	0	0	1.4	2	SH1	0.25	0.25	0	0	1.3	1
	SH7	3.5	5.3	2.2	0	3.4	6	SH1	0.25	0.25	0	0	1.3	1
	SH8	2.05	3.4	0.85	0	4.35	3	SH1	0.25	0.25	0	0	1.3	1
	SH9	4.5	2.45	0	1.55	7	4.4	SH1	0.25	0.25	0	0.15	1.3	1
Timber Understory	TU1	0.2	0.9	1.5	0.2	0.9	0.6	TU1	0.2	0.9	1.5	0.2	0.9	0.6
	TU2	0.95	1.8	1.25	0	0.2	1	TU1	0.2	0.9	1.25	0	0.2	0.6
	TU3	1.1	0.15	0.25	0.65	1.1	1.3	TU1	0.2	0.15	0.25	0.2	0.9	0.6
	TU4	4.5	0	0	0	2	0.5	TU1	0.2	0	0	0	0.9	0.5

	TU5	4	4	3	0	3	1	TU1	0.2	0.9	1.5	0	0.9	0.6
Timber Litter	TL1	1	2.2	3.6	0	0	0.2	TL1	1	2.2	3.6	0	0	0.2
	TL2	1.4	2.3	2.2	0	0	0.2	TL1	1	2.2	2.2	0	0	0.2
	TL3	0.5	2.2	2.8	0	0	0.3	TL1	0.5	2.2	2.8	0	0	0.2
	TL4	0.5	1.5	4.2	0	0	0.4	TL1	0.5	1.5	3.6	0	0	0.2
	TL5	1.15	2.5	4.4	0	0	0.6	TL1	1	2.2	3.6	0	0	0.2
	TL6	2.4	1.2	1.2	0	0	0.3	TL1	1	1.2	1.2	0	0	0.2
	TL7	0.3	1.4	8.1	0	0	0.4	TL1	0.3	1.4	3.6	0	0	0.2
	TL8	5.8	1.4	1.1	0	0	0.3	TL1	1	1.4	1.1	0	0	0.2
	TL9	6.65	3.3	4.15	0	0	0.6	TL1	1	2.2	3.6	0	0	0.2
Slash-Blowdown	SB1	0	15	0	0	0	1	SB1	0	15	0	0	0	1
	SB2	10	0	0	0	0	1	SB1	0	0	0	0	0	1
	SB3	10	0	0	0	0	1.5	SB1	0	0	0	0	0	1
	SB4	10	0	0	0	0	1.5	SB1	0	0	0	0	0	1
Non-Burnable	NB1	0	0	0	0	0	0	NB1	0	0	0	0	0	0
	NB2	0	0	0	0	0	0	NB2	0	0	0	0	0	0
	NB3	0	0	0	0	0	0	NB3	0	0	0	0	0	0
	NB8	0	0	0	0	0	0	NB8	0	0	0	0	0	0
	NB9	0	0	0	0	0	0	NB9	0	0	0	0	0	0

Extended Data Table 4: Hyperparameters used in the thirty machine learning models.

Neural Network									Random Forest					
NumLayers	Activations	Standardize	Lambda	LayerWeightsInitializer	LayerBiasesInitializer	Layer_1_Size	Layer_2_Size	Layer_3_Size	MinLeafSize	MaxNumSplits	NumVariablesToSample	Method	NumLearningCycles	LearnRate
2	sigmoid	TRUE	5.14343E-10	he	ones	94	59		3	3750	4	Bag	341	
2	tanh	FALSE	0.593086789	glorot	ones	73	38		2	3496	4	LSBoost	60	0.101086
2	tanh	TRUE	0.062738436	glorot	zeros	293	6		7	2473	5	Bag	430	
1	tanh	FALSE	0.009311794	glorot	zeros	101			18	14294	10	Bag	11	
3	sigmoid	TRUE	1.93908E-09	glorot	zeros	3	2	9	8	4608	2	LSBoost	286	0.040545
1	relu	TRUE	1.29452E-08	glorot	zeros	2			5	22130	5	Bag	139	
1	sigmoid	TRUE	0.094512392	he	zeros	243			2	4501	4	Bag	95	
1	relu	FALSE	4.495E-10	glorot	zeros	232			3	26193	3	Bag	490	
1	sigmoid	TRUE	0.712843234	glorot	ones	89			3	2344	8	Bag	394	
3	sigmoid	TRUE	3.69926E-10	he	ones	55	19	70	3	6032	7	Bag	143	
2	tanh	FALSE	1.339920887	glorot	zeros	27	82		12	202	2	LSBoost	64	0.105735
2	tanh	TRUE	0.712009205	he	ones	25	167		10	16985	9	Bag	67	
3	tanh	TRUE	2.244015242	he	ones	4	27	87	2	2335	2	Bag	391	
2	sigmoid	TRUE	0.139426304	glorot	zeros	185	3		16	20191	10	Bag	18	
2	sigmoid	FALSE	1.537153126	he	ones	295	13		3	21621	5	Bag	183	

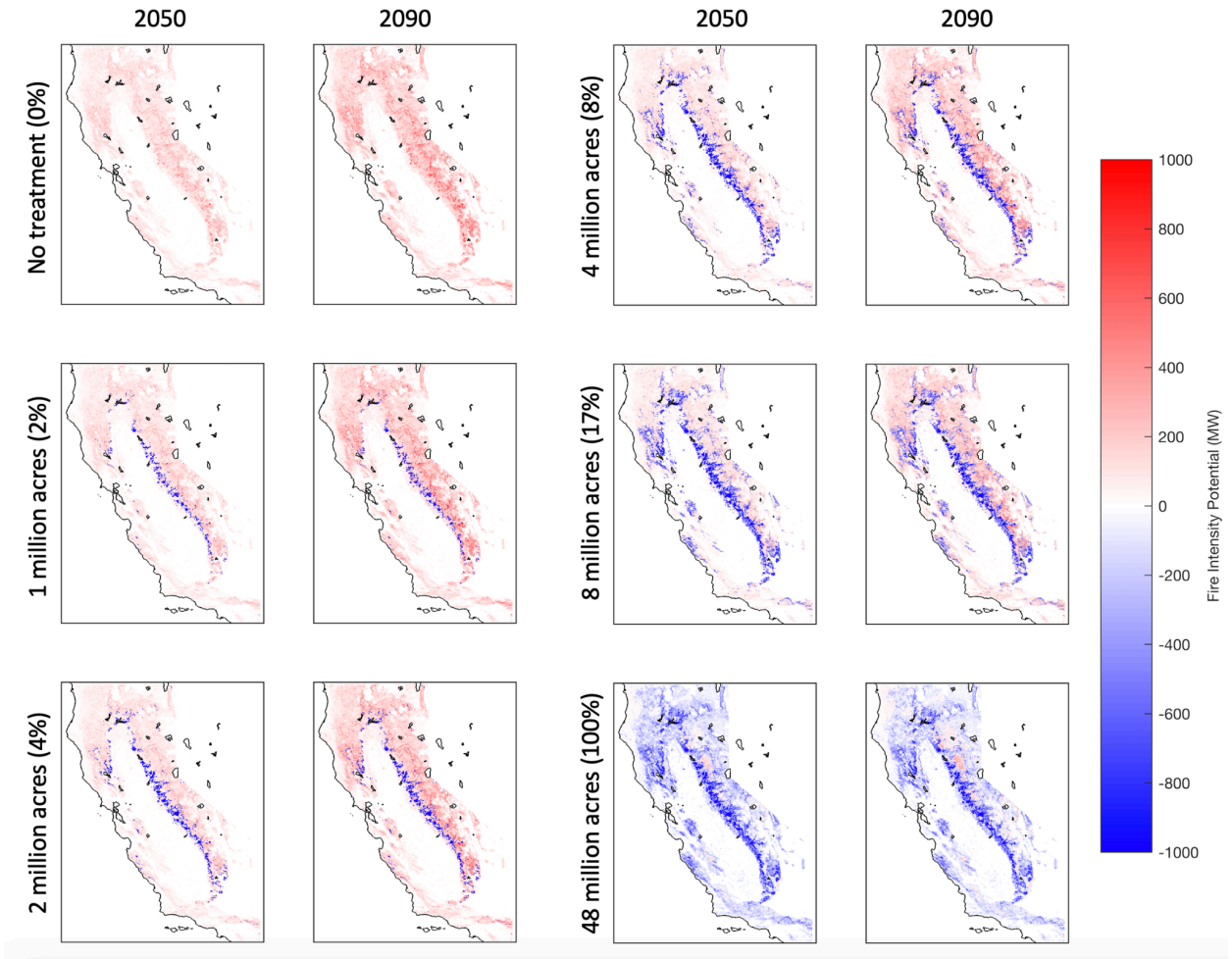

Extended Data Fig. 3: Difference in FIP for the thirty most consequential weather snapshots between today's climatological temperature and that in 2050 and 2090 under six levels of targeted fuel treatment extent. If fuel reduction were maintained at a frequency of once every five years, the intermediate scenarios would correspond to treatment rates of 200,000 acres/year (0.4% of our domain), 400,000 acres/year (0.8% of our domain), 800,000 acres/year (1.7% of our domain), and 1,600,000 acres/year (~3% of our domain). See extended Data Fig. 4 for the effects of these targeted treatments on domain-mean FIPs.

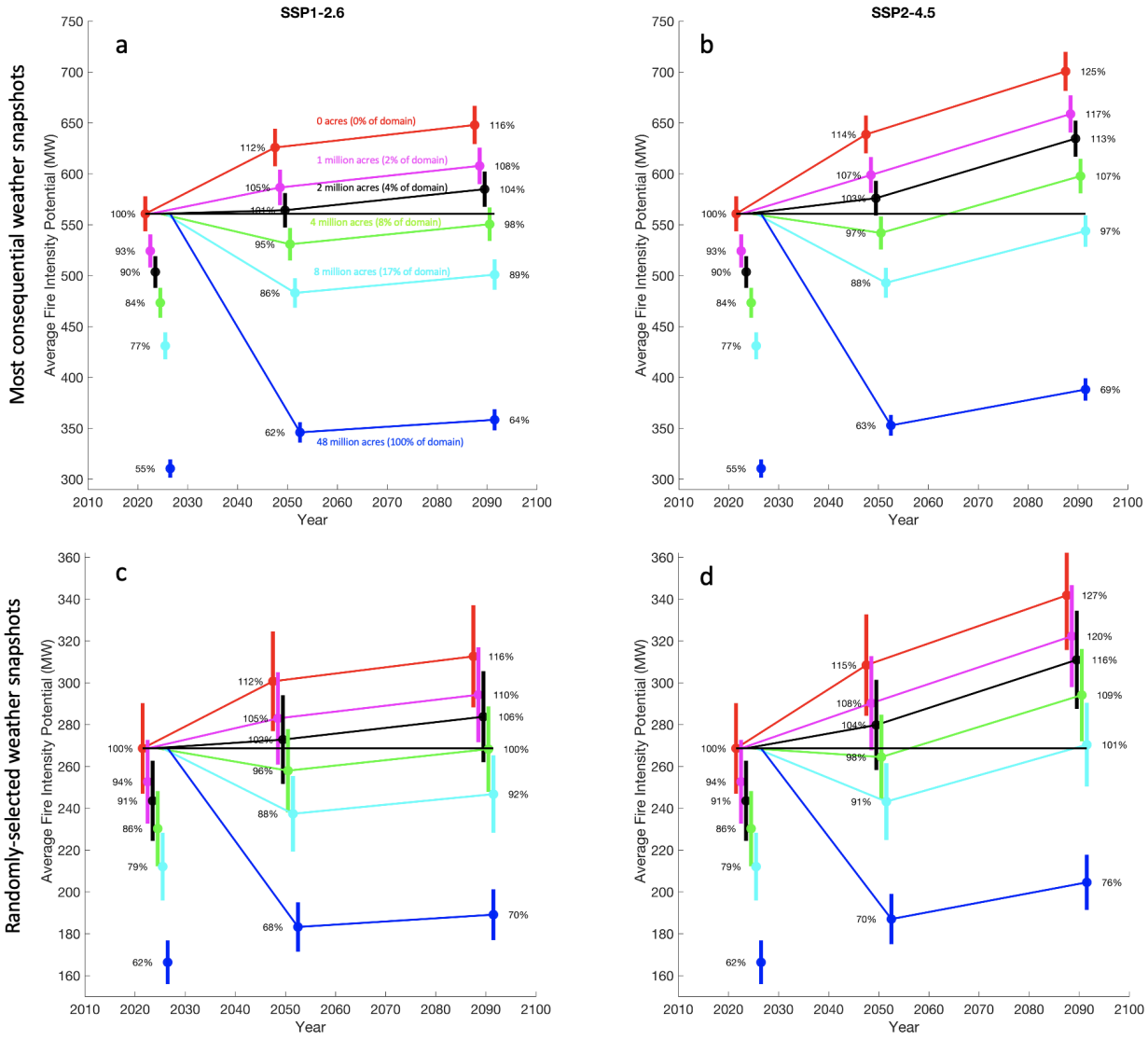

Extended Data Fig. 4: Same as Fig. 4a and 4b but for all the treatment extent scenarios. **a,b,** for the thirty most consequential weather snapshots, and **c,d** for the thirty random weather snapshots. **a,c** for the SSP1-2.6 scenario and **b,d** for the SSP2-4.5 scenario.

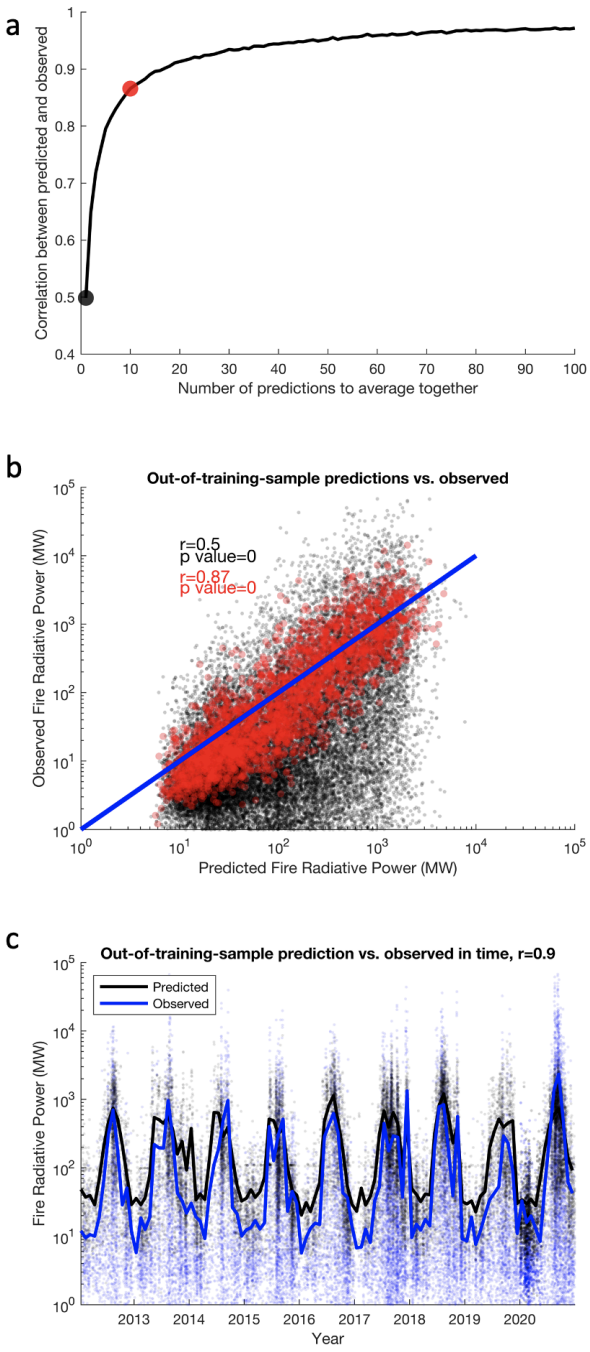

Extended Data Fig. 5: Validation of machine learning predictions on out-of-training-sample data using leave-one-year-out cross-validation. a, correlation in log space between model ensemble median predictions (median across thirty machine learning models) and observations as a function of the number of predictions averaged together. **b,** scatterplots of ensemble median predictions and observations without any averaging of multiple predictions (black) and for averaging ten predictions together (red). **c**, all observations (blue) and predictions (black) represented in time (dots) as well as monthly mean values (lines). The correlation at the monthly mean level between predictions and observations is r=0.9.

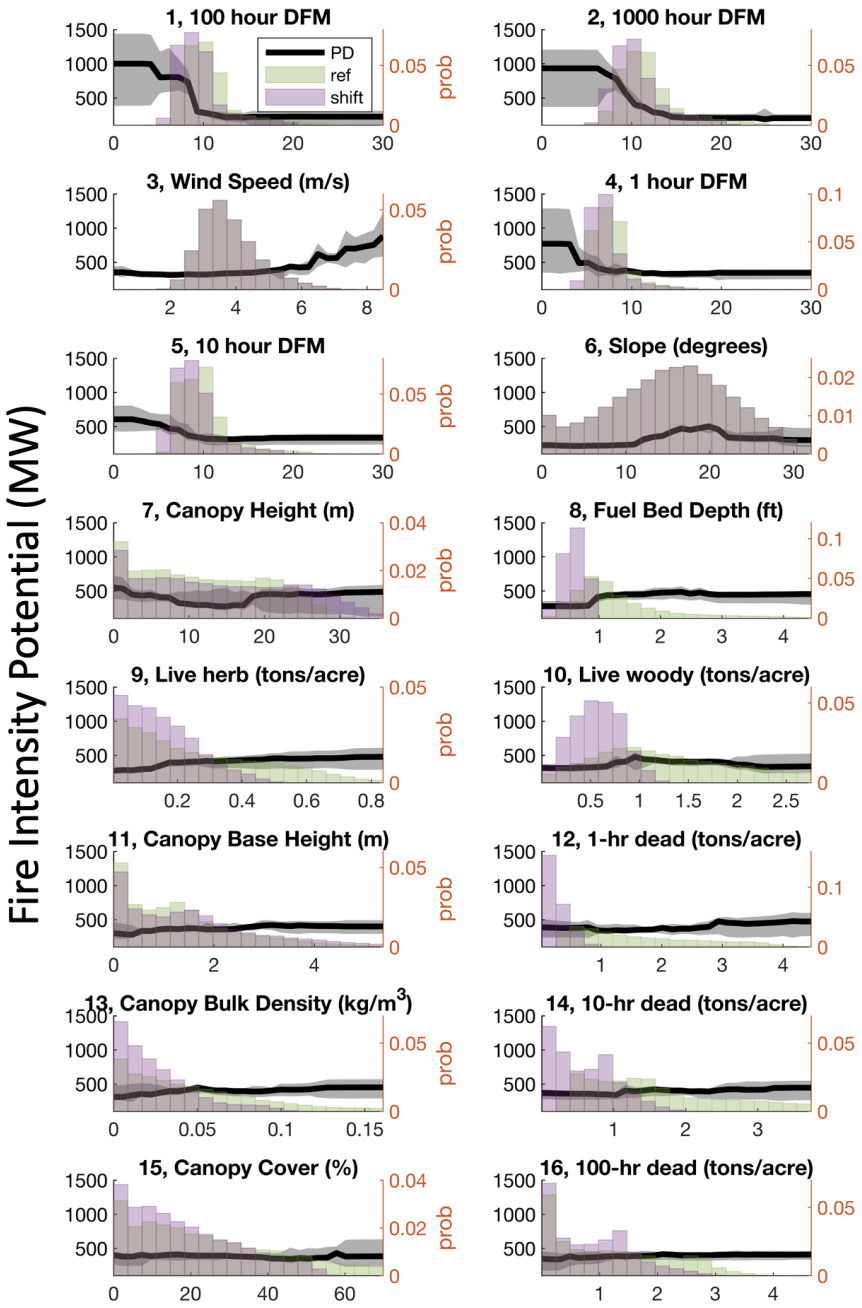

Extended Data Fig. 6: The partial dependence of each predictor and the shift in their distributions under the climate change and fuel reduction scenarios. Black lines are the partial dependence functions (https://www.mathworks.com/help/stats/regressiontree.partialdependence.html) averaged over the machine learning models (with standard deviations shown in gray). The two distributions represent the reference distribution without any alteration and a shifted distribution. The shifted distribution corresponds to the effect of climate change for the weather/climate variables (1, 10, 100, and 1,000 dead fuel moisture), and it represents hazardous fuel reduction treatments for the fuel characteristics.

Acknowledgments: We acknowledge the Pacific Gas and Electric Meteorology Operations and Fire Science Team for guidance and discussion throughout the project. We acknowledge teams at DTN (https://www.dtn.com/), Technosylva (https://technosylva.com/), and Sonoma Technology (http://www.sonomatech.com/) for data preprocessing and preparation. We also acknowledge Erica Turner, Mike Voss, and Evan Duffey for valuable discussions.

Funding and conflicts of interest: This project was partially funded from a contract (#C6909) between The San José State University Research Foundation and Pacific Gas and Electric (PG&E) titled "Understanding Extreme Fire Weather Conditions using a 30-year High-Resolution WRF Model Dataset" in which PG&E provided data and operational fire weather expertise to scientists affiliated with San Jose State's Wildfire Interdisciplinary Research Center (WIRC). There were no financial conflicts of interest in the production of this study. Nevertheless, this section allows us to address potential *perceived* conflicts of interest, which may be possible given PG&E's financial liability for past wildfires. PG&E coauthors of this study Scott J. Strenfel and Richard B. Bagley are in the Meteorology Operations and Fire Science division of PG&E, where Scott J. Strenfel is the division Director. Their primary interest related to this project is to improve PG&E's internal fire potential index (similar to the FIP of this study), which is used to inform operational decisions like whether to execute public safety power shutoffs. Another PG&E interest is the spatial pattern of fire risk under climate change scenarios (i.e., our future FIP maps), which could help inform the prioritization of grid hardening. These interests are not *in conflict* (financial or otherwise) but instead are well-aligned with objectively addressing the research questions laid out in this study, so there are no conflicts of interest to report.

Data availability: The Weather Research and Forecasting (WRF) model used for the predictor data is open source and can be downloaded at https://github.com/wrf-model/WRF/releases. The fuel data from LandFire can be downloaded at https://landfire.gov/, the VIIRS fire products that were used for the response data can be downloaded at https://viirsland.gsfc.nasa.gov/Products/NASA/FireESDR.html, and the CORDEX climate model data can be downloaded at https://interactive-atlas.ipcc.ch/regional-information.

Code availability: Code for this study is archived at https://github.com/ptbrown31/The-Potential-for-Fuel-Reduction-to-Counteract-Climate-Warming/tree/main

Reference list

1 Jain, P., Castellanos-Acuna, D., Coogan, S. C. P., Abatzoglou, J. T. & Flannigan, M. D. Observed increases in extreme fire weather driven by atmospheric humidity and temperature. *Nature Climate Change* **12** , 63-70 (2022). https://doi.org/10.1038/s41558-021-01224-1

2 Abatzoglou, J. T. & Williams, A. P. Impact of anthropogenic climate change on wildfire across western US forests. *Proceedings of the National Academy of Sciences* **113** , 11770-11775

(2016). https://doi.org/10.1073/pnas.1607171113

3 Brown, P. T. *et al.* Climate warming increases extreme daily wildfire growth risk in California. *Nature* **621** , 760-766 (2023). https://doi.org/10.1038/s41586-023-06444-3

4 Williams, A. P. *et al.* Observed Impacts of Anthropogenic Climate Change on Wildfire in California. *Earth's Future* **7** , 892-910 (2019). https://doi.org/10.1029/2019ef001210

5 US Department of Agriculture Forest Service, "Confronting the wildfire crisis: A strategy for protecting communities and improving resilience in America's forests" (FS-1187a, US Department of Agriculture Forest Service, 2022); www.fs.usda.gov/sites/default/files/Confronting-Wildfire-Crisis.pdf.

6 California Wildfire and Forest Resilience Task Force, California's Wildfire and Forest Resilience Action Plan (California Wildfire and Forest Resilience Task Force, 2021); https://www.wildfiretaskforce.org/wp-content/uploads/2022/04/californiawildfireandforestresilienceactionplan.pdf.

7 Stephens, S. L., Martin, R. E. & Clinton, N. E. Prehistoric fire area and emissions from California's forests, woodlands, shrublands, and grasslands. *Forest Ecology and Management* **251** , 205-216 (2007). https://doi.org/10.1016/j.foreco.2007.06.005

8 Marlon, J. R. *et al.* Long-term perspective on wildfires in the western USA. *Proceedings of the National Academy of Sciences* **109** , E535-E543 (2012). https://doi.org/10.1073/pnas.1112839109

9 Bowman, D. M. J. S. *et al.* Vegetation fires in the Anthropocene. *Nature Reviews Earth & Environment* **1** , 500-515 (2020). https://doi.org/10.1038/s43017-020-0085-3

10 Burke, M. *et al.* The changing risk and burden of wildfire in the United States. *Proceedings of the National Academy of Sciences* **118** , e2011048118 (2021). https://doi.org/10.1073/pnas.2011048118

11 Jones, M. W. *et al.* Global and Regional Trends and Drivers of Fire Under Climate Change. *Reviews of Geophysics* **60** (2022). https://doi.org/10.1029/2020rg000726

12 Turco, M. *et al.* Anthropogenic climate change impacts exacerbate summer forest fires in California. *Proceedings of the National Academy of Sciences* **120** (2023). https://doi.org/10.1073/pnas.2213815120

13 Paci, J. N., M; Gage, T. The Economic, Fiscal, and Environmental Costs of Wildfires in California. (Gordon and Betty Moore Foundation, 2023).

14 Wang, D. *et al.* Economic footprint of California wildfires in 2018. *Nature Sustainability* (2020). https://doi.org/10.1038/s41893-020-00646-7

15 Starrs, C. F., Butsic, V., Stephens, C. & Stewart, W. The impact of land ownership, firefighting, and reserve status on fire probability in California. *Environmental Research Letters* **13** , 034025 (2018). https://doi.org/10.1088/1748-9326/aaaad1

16 Syphard, A. D., Keeley, J. E., Pfaff, A. H. & Ferschweiler, K. Human presence diminishes the importance of climate in driving fire activity across the United States. *Proceedings of the National Academy of Sciences* **114** , 13750-13755 (2017). https://doi.org/10.1073/pnas.1713885114

17 Balch, J. K. *et al.* Human-started wildfires expand the fire niche across the United States. *Proceedings of the National Academy of Sciences* **114** , 2946-2951 (2017). https://doi.org/10.1073/pnas.1617394114

18 Nagy, R. C., Fusco, E., Bradley, B., Abatzoglou, J. T. & Balch, J. Human-Related Ignitions Increase the Number of Large Wildfires across U.S. Ecoregions. *Fire* **1** , 4 (2018). https://doi.org/10.3390/fire1010004

19 Radeloff, V. C. *et al.* Rapid growth of the US wildland-urban interface raises wildfire risk. *Proceedings of the National Academy of Sciences* **115** , 3314-3319 (2018). https://doi.org/10.1073/pnas.1718850115

20 Radeloff, V. C. *et al.* Rising wildfire risk to houses in the United States, especially in grasslands and shrublands. *Science* **382** , 702-707 (2023). https://doi.org/doi:10.1126/science.ade9223

21 Safford, D. H. & Water, D. V. M. K. Using fire return interval departure (FRID) analysis to map spatial and temporal changes in fire frequency on national forest lands in California. 59 (Albany, CA: U.S. Department of Agriculture, Forest Service, Pacific Southwest Research Station, 2014).

22 Collins, M. B., Miller, D. J., Knapp, E. E. & Sapsis, B. D. A quantitative comparison of forest fires in central and northern California under early (1911–1924) and contemporary (2002–2015) fire suppression. *International Journal of Wildland Fire* **28** , 138 (2019). https://doi.org/https://doi.org/10.1071/WF18137

23 Boisramé, G. F. S., Brown, T. J. & Bachelet, D. M. Trends in western USA fire fuels using historical data and modeling. *Fire Ecology* **18** (2022). https://doi.org/10.1186/s42408-022-00129-4

24 Graham, T. R., Mccaffrey, S. & Jain, B. T. Science basis for changing forest structure to modify wildfire behavior and severity. 43 (Fort Collins, CO: U.S. Department of Agriculture, Forest Service, Rocky Mountain Research Station, 2004).

25 Knight, C. A. *et al.* Land management explains major trends in forest structure and composition over the last millennium in California's Klamath Mountains. *Proceedings of the National Academy of Sciences* **119** (2022). https://doi.org/10.1073/pnas.2116264119

26 Reinhardt, D. E., Keane, E. R., Calkin, E. D. & Cohen, D. J. Objectives and considerations for wildland fuel treatment in forested ecosystems of the interior western United States. *Forest Ecology and Management* **256** , 1997-2006 (2008). https://doi.org/https://doi.org/10.1016/j.foreco.2008.09.016

27 Clark, E. P., Porter, A. B., Pellant, M., Dyer, K. & Norton, P. T. Evaluating the Efficacy of Targeted Cattle Grazing for Fuel Break Creation and Maintenance. *Rangeland Ecology & Management* **89** , 69-86 (2023). https://doi.org/https://doi.org/10.1016/j.rama.2023.02.005

28 Beebe, G. R., Knapp, L. S. P., Stambaugh, M. C., Davidson, B. K. & Dey, D. C. Smoke, goats, and oaks: Effects of goat browsing and prescribed fire on woodland structure and floristic composition in Ozark hardwoods. 4 (Fort Collins, CO: U.S. Department of Agriculture, Forest Service, Rocky Mountain Research Station, 2022).

29 Ott, J. E., Kilkenny, F. F. & Jain, T. B. Fuel treatment effectiveness at the landscape scale: a systematic review of simulation studies comparing treatment scenarios in North America. *Fire Ecology* **19** (2023). https://doi.org/10.1186/s42408-022-00163-2

30 Taylor, A. H., Harris, L. B. & Skinner, C. N. Severity patterns of the 2021 Dixie Fire exemplify the need to increase low-severity fire treatments in California's forests. *Environmental Research Letters* **17** , 071002 (2022). https://doi.org/10.1088/1748-9326/ac7735

31 Evans, S. G. *et al.* Modeling the Risk Reduction Benefit of Forest Management Using a Case Study in the Lake Tahoe Basin. *Ecology and Society* **27** (2022). https://doi.org/10.5751/es-13169-270218

32 Vaillant, N. M., Fites-Kaufman, J., Reiner, A. L., Noonan-Wright, E. K. & Dailey, S. N. Effect of Fuel Treatments on Fuels and Potential Fire Behavior in California, USA, National Forests. *Fire Ecology* **5** , 14-29 (2009). https://doi.org/10.4996/fireecology.0502014

33 Pollet, J. & Omi, N. P. Effect of thinning and prescribed burning on crown fire severity in ponderosa pine forests. *International Journal of Wildland Fire* **11** , 1 (2002). https://doi.org/https://doi.org/10.1071/WF01045

34 Agee, J. K. & Lolley, M. R. Thinning and Prescribed Fire Effects on Fuels and Potential Fire Behavior in an Eastern Cascades Forest, Washington, USA. *Fire Ecology* **2** , 3-19 (2006). https://doi.org/10.4996/fireecology.0202003

35 Prichard, J. S., Peterson, L. D. & Jacobson, K. Fuel treatments reduce the severity of wildfire effects in dry mixed conifer forest, Washington, USA. *Canadian Journal of Forest Research* **40** , 1615-1626 (2010). https://doi.org/https://doi.org/10.1139/X10-109

36 Krofcheck, D. J., Hurteau, M. D., Scheller, R. M. & Loudermilk, E. L. Restoring surface fire stabilizes forest carbon under extreme fire weather in the Sierra Nevada. *Ecosphere* **8** , e01663 (2017). https://doi.org/10.1002/ecs2.1663

37 Prichard, S. J. *et al.* Adapting western North American forests to climate change and wildfires: 10 common questions. *Ecological Applications* **31** (2021). https://doi.org/10.1002/eap.2433

38 [Anon]. *Gov. Newsom AB179, the Budget Act of 2022 EXPENDITURE PLAN* , < https://wildfiretaskforce.org/about/expenditure-plan/ > (2022).

39 Mckinney, S. T., Abrahamson, I., Jain, T. & Anderson, N. A systematic review of empirical evidence for landscape-level fuel treatment effectiveness. *Fire Ecology* **18** (2022). https://doi.org/10.1186/s42408-022-00146-3

40 Kloster, S. & Lasslop, G. Historical and future fire occurrence (1850 to 2100) simulated in CMIP5 Earth System Models. *Global and Planetary Change* **150** , 58-69 (2017). https://doi.org/https://doi.org/10.1016/j.gloplacha.2016.12.017

41 Wooster, M. J., Roberts, G., Perry, G. L. W. & Kaufman, Y. J. Retrieval of biomass combustion rates and totals from fire radiative power observations: FRP derivation and calibration relationships between biomass consumption and fire radiative energy release. *Journal of Geophysical Research: Atmospheres* **110** (2005). https://doi.org/10.1029/2005jd006318

42 Ichoku, C., Giglio, L., Wooster, J. M. & Remer, A. L. Global characterization of biomass-burning patterns using satellite measurements of fire radiative energy. *Remote Sensing of Environment* **112** , 2950-2962 (2008). https://doi.org/https://doi.org/10.1016/j.rse.2008.02.009

43 Ichoku, C. & Ellison, L. Global top-down smoke-aerosol emissions estimation using satellite fire radiative power measurements. *Atmospheric Chemistry and Physics* **14** , 6643-6667 (2014). https://doi.org/10.5194/acp-14-6643-2014

44 Tang, W. & Arellano, A. F. Investigating dominant characteristics of fires across the Amazon during 2005–2014 through satellite data synthesis of combustion signatures. *Journal of Geophysical Research: Atmospheres* **122** , 1224-1245 (2017). https://doi.org/10.1002/2016jd025216

45 Laurent, P., Mouillot, F., Moreno, M. V., Yue, C. & Ciais, P. Varying relationships between fire radiative power and fire size at a global scale. *Biogeosciences* **16** , 275-288 (2019). https://doi.org/10.5194/bg-16-275-2019

46 Balch, K. J. *et al.* Warming weakens the night-time barrier to global fire. *Nature* **602** , 442-448 (2022). https://doi.org/https://doi.org/10.1038/s41586-021-04325-1

47 Bond, W. & Keeley, J. Fire as a global 'herbivore': the ecology and evolution of flammable ecosystems. *Trends in Ecology & Evolution* **20** , 387-394 (2005). https://doi.org/https://doi.org/10.1016/j.tree.2005.04.025

48 Wu, X., Sverdrup, E., Mastrandrea, M. D., Wara, M. W. & Wager, S. Low-intensity fires mitigate the risk of high-intensity wildfires in California's forests. *Science Advances* **9** (2023). https://doi.org/10.1126/sciadv.adi4123

49 Collins, M. B. *et al.* Modeling hazardous fire potential within a completed fuel treatment network in the northern Sierra Nevada. *Forest Ecology and Management* **310** , 156-166 (2013). https://doi.org/https://doi.org/10.1016/j.foreco.2013.08.015

50 Fernández-Guisuraga, J. M. & Fernandes, P. M. Prescribed burning mitigates the severity of subsequent wildfires in Mediterranean shrublands. *Fire Ecology* **20** (2024). https://doi.org/10.1186/s42408-023-00233-z

51 Meinshausen, M. *et al.* The shared socio-economic pathway (SSP) greenhouse gas concentrations and their extensions to 2500. *Geoscientific Model Development* **13** , 3571-3605 (2020). https://doi.org/https://doi.org/10.5194/gmd-13-3571-2020

52 Riahi, K. *et al.* The Shared Socioeconomic Pathways and their energy, land use, and greenhouse gas emissions implications: An overview. *Global Environmental Change* **42** , 153-168 (2017). https://doi.org/https://doi.org/10.1016/j.gloenvcha.2016.05.009

53 Sleeter, B. M., Wilson, T. S., Sharygin, E. & Sherba, J. T. Future Scenarios of Land Change Based on Empirical Data and Demographic Trends. *Earth's Future* **5** , 1068-1083 (2017).

https://doi.org/10.1002/2017ef000560

54 Hurteau, M. D., Liang, S., Westerling, A. L. & Wiedinmyer, C. Vegetation-fire feedback reduces projected area burned under climate change. *Scientific Reports* **9** (2019). https://doi.org/10.1038/s41598-019-39284-1

55 Walker, X. J. *et al.* Fuel availability not fire weather controls boreal wildfire severity and carbon emissions. *Nature Climate Change* **10** , 1130-1136 (2020). https://doi.org/10.1038/s41558-020-00920-8

56 Abatzoglou, J. T. *et al.* Projected increases in western US forest fire despite growing fuel constraints. *Communications Earth & Environment* **2** (2021). https://doi.org/10.1038/s43247-021-00299-0

57 Swain, D. L. *et al.* Climate change is narrowing and shifting prescribed fire windows in western United States. *Communications Earth & Environment* **4** (2023). https://doi.org/10.1038/s43247-023-00993-1

58 Williams, N. J. *et al.* Overcoming obstacles to prescribed fire in the North American Mediterranean climate zone. *Frontiers in Ecology and the Environment* **22** (2024). https://doi.org/https://doi.org/10.1002/fee.2687

59 Prichard, J. S., Povak, A. N., Kennedy, C. M. & Peterson, W. D. Fuel treatment effectiveness in the context of landform, vegetation, and large, wind‐driven wildfires. *Ecological Applications* **30** (2020). https://doi.org/https://doi.org/10.1002/eap.2104

60 G Barros, A. M., Ager, A. A., Day, M. A. & Palaiologou, P. Improving long-term fuel treatment effectiveness in the National Forest System through quantitative prioritization. *Forest Ecology and Management* **433** , 514-527 (2019). https://doi.org/10.1016/j.foreco.2018.10.041

61 Krofcheck, D. J., Hurteau, M. D., Scheller, R. M. & Loudermilk, E. L. Prioritizing forest fuels treatments based on the probability of high‐severity fire restores adaptive capacity in Sierran forests. *Global Change Biology* **24** , 729-737 (2018). https://doi.org/10.1111/gcb.13913

62 Alcasena, F., Ager, A. A., Belavenutti, P., Krawchuk, M. & Day, A. M. Contrasting the efficiency of landscape versus community protection fuel treatment strategies to reduce wildfire exposure and risk. *Journal of Environmental Management* **309** , 114650 (2022). https://doi.org/https://doi.org/10.1016/j.jenvman.2022.114650

63 Tubbesing, C. L. *et al.* Strategically placed landscape fuel treatments decrease fire

severity and promote recovery in the northern Sierra Nevada. *Forest Ecology and Management* **436** , 45-55 (2019). https://doi.org/10.1016/j.foreco.2019.01.010

64 Schmidt, A. D., Taylor, H. A. & Skinner, N. C. The influence of fuels treatment and landscape arrangement on simulated fire behavior, Southern Cascade range, California. *Forest Ecology and Management* **255** , 3170-3184 (2008). https://doi.org/https://doi.org/10.1016/j.foreco.2008.01.023

65 Kim, Y.-H., Bettinger, P. & Finney, M. Spatial optimization of the pattern of fuel management activities and subsequent effects on simulated wildfires. *European Journal of Operational Research* **197** , 253-265 (2009). https://doi.org/https://doi.org/10.1016/j.ejor.2008.05.025

66 Safford, H. D., Stevens, J. T., Merriam, K., Meyer, M. D. & Latimer, A. M. Fuel treatment effectiveness in California yellow pine and mixed conifer forests. *Forest Ecology and Management* **274** , 17-28 (2012). https://doi.org/https://doi.org/10.1016/j.foreco.2012.02.013

67 Stephens, L. S. *et al.* The Effects of Forest Fuel-Reduction Treatments in the United States. *BioScience* **62** , 549-560 (2012). https://doi.org/https://doi.org/10.1525/bio.2012.62.6.6

68 Jones, M. G. *et al.* Forest restoration limits megafires and supports species conservation under climate change. *Frontiers in Ecology and the Environment* **20** , 210-216 (2022). https://doi.org/https://doi.org/10.1002/fee.2450

69 North, P. M. *et al.* Pyrosilviculture Needed for Landscape Resilience of Dry Western United States Forests. *Journal of Forestry* **119** , 520-544 (2021). https://doi.org/https://doi.org/10.1093/jofore/fvab026

70 Wang, S. S. C., Qian, Y., Leung, L. R. & Zhang, Y. Identifying Key Drivers of Wildfires in the Contiguous US Using Machine Learning and Game Theory Interpretation. *Earth's Future* **9** (2021). https://doi.org/10.1029/2020ef001910

71 Huang, Y., Jin, Y., Schwartz, M. W. & Thorne, J. H. Intensified burn severity in California's northern coastal mountains by drier climatic condition. *Environmental Research Letters* **15** , 104033 (2020). https://doi.org/10.1088/1748-9326/aba6af

72 Elia, M. *et al.* Estimating the probability of wildfire occurrence in Mediterranean landscapes using Artificial Neural Networks. *Environmental Impact Assessment Review* **85** , 106474 (2020). https://doi.org/10.1016/j.eiar.2020.106474

73 Kondylatos, S. *et al.* Wildfire Danger Prediction and Understanding With Deep Learning. *Geophysical Research Letters* **49** (2022). https://doi.org/10.1029/2022gl099368

74 Satir, O., Berberoglu, S. & Donmez, C. Mapping regional forest fire probability using artificial neural network model in a Mediterranean forest ecosystem. *Geomatics, Natural Hazards and Risk* **7** , 1645-1658 (2016). https://doi.org/10.1080/19475705.2015.1084541

75 Schroeder, W., Oliva, P., Giglio, L. & Csiszar, A. I. The New VIIRS 375 m active fire detection data product: Algorithm description and initial assessment. *Remote Sensing of Environment* **143** , 85-96 (2014). https://doi.org/https://doi.org/10.1016/j.rse.2013.12.008

76 Mcclure, D. C., Pavlovic, R. N., Huang, S., Chaveste, M. & Wang, N. Consistent, high-accuracy mapping of daily and sub-daily wildfire growth with satellite observations. *International Journal of Wildland Fire* **32** , 694-708 (2023). https://doi.org/https://doi.org/10.1071/WF22048

77 Rollins, G. M. LANDFIRE: a nationally consistent vegetation, wildland fire, and fuel assessment. *International Journal of Wildland Fire* **18** , 235 (2009). https://doi.org/https://doi.org/10.1071/WF08088

78 Joseph, M. B. *et al.* Spatiotemporal prediction of wildfire size extremes with Bayesian finite sample maxima. *Ecological Applications* **29** , e01898 (2019). https://doi.org/10.1002/eap.1898

79 Gutierrez, A. A. *et al.* Wildfire response to changing daily temperature extremes in California's Sierra Nevada. *Science Advances* **7** (2021). https://doi.org/DOI : 10.1126/sciadv.abe6 417

80 Urza, K. A., Hanberry, B. B. & Jain, B. T. Landscape-scale fuel treatment effectiveness: lessons learned from wildland fire case studies in forests of the western United States and Great Lakes region. *Fire Ecology* **19** (2023). https://doi.org/https://doi.org/10.1186/s42408-022-00159-y

81 Moritz, M. A., Morais, M. E., Summerell, L. A., Carlson, J. M. & Doyle, J. Wildfires, complexity, and highly optimized tolerance. *Proceedings of the National Academy of Sciences of the United States of America* **102** , 17912-17917 (2005). https://doi.org/10.1073/pnas.0508985102

82 Werth, P. A. B. E. P. M. E. A. M. G. C. C. B. C. M. A. F. J. M. F. Synthesis of Knowledge of Extreme Fire Behavior: Volume 2 for Fire Behavior Specialists, Researchers, and Meteorologists. (U.S. Forest Service, General Technical Report PNW-GTR-891, 2016).

83 Ryan, C. K. *et al.* Landfire: National vegetation and fuel mapping for fire management planning. *Forest Ecology and Management* **234** , S220 (2006). https://doi.org/https://doi.org/10.1016/j.foreco.2006.08.247

84 Xiao, J. *et al.* Remote sensing of the terrestrial carbon cycle: A review of advances over 50 years. *Remote Sensing of Environment* **233** , 111383 (2019). https://doi.org/https://doi.org/10.1016/j.rse.2019.111383

85 Mcnorton, R. J. & Giuseppe, D. F. A global fuel characteristic model and dataset for wildfire prediction. *Biogeosciences* **21** , 279-300 (2024). https://doi.org/https://doi.org/10.5194/bg-21-279-2024

86 Scott, H. J. & Burgan, E. R. Standard fire behavior fuel models: a comprehensive set for use with Rothermel's surface fire spread model. 72 (Fort Collins, CO: U.S. Department of Agriculture, Forest Service, Rocky Mountain Research Station, 2005).

87 Mcevoy, J. D., Pierce, W. D., Kalansky, F. J., Cayan, R. D. & Abatzoglou, T. J. Projected Changes in Reference Evapotranspiration in California and Nevada: Implications for Drought and Wildland Fire Danger. *Earth's Future* **8** (2020). https://doi.org/https://doi.org/10.1029/2020EF001736

88 Mandel, J. *et al.* Recent advances and applications of WRF–SFIRE. *Natural Hazards and Earth System Sciences* **14** , 2829-2845 (2014). https://doi.org/10.5194/nhess-14-2829-2014

89 Dillon, G. K., Menakis, J. & Fay, F. Wildland fire potential: A tool for assessing wildfire risk and fuels management needs. 60-76 (Fort Collins, CO: U.S. Department of Agriculture, Forest Service, Rocky Mountain Research Station, 2015).

90 Gannon, B. Chaffee County Fuel Treatment Prioritization. (Colorado Forest Restoration Institute. CFRI-1914, 2019). https://cfri.colostate.edu/2020/02/10/new-publications-chaffee-county-wildfire-risk-assessment-and-fuel-treatment-prioritization/